INVITED PAPER

Integrated Electricity–Heat–Gas Systems: Techno–Economic Modeling, Optimization, and Application to Multienergy Districts

This article is a tutorial on modeling and simulations of a multienergy system containing a portfolio of integrated electricity and gas distribution and district heating subsystems.

By Eduardo Alejandro Martínez Ceseña, *Member IEEE*, Emmanouil Loukarakis, Nicholas Good, and Pierluigi Mancarella, *Senior Member IEEE*

ABSTRACT | Multienergy systems (MES) can optimally deploy their internal operational flexibility to use combinations of different energy vectors to meet the needs of end-users and potentially support the wider system. Key relevant applications of MES are multienergy districts (MEDs) with, for example, integrated electricity and gas distribution and district heating networks. Simulation and optimization of MEDs is a grand challenge requiring sophisticated techno–economic tools that are capable of modeling buildings and distributed energy resources (DERs) across multienergy networks. This article provides a tutorial-like overview of the state-of-the-art concepts for techno–economic modeling and optimization of integrated electricity–heat–gas systems in flexible MEDs, also considering operational uncertainty and multiple grid support services. Relevant mixed integer linear programming (MILP) formulations for two-stage stochastic scheduling of buildings and DER, iteratively soft-coupled to nonlinear network models, are then presented as the basis of a practical network-constrained MED energy management tool developed in several projects. The concepts presented are demonstrated through real-world applications based on The University of Manchester MED case study, the details of which are also provided as a testbed for future research.

KEYWORDS | Integrated electricity–heat–gas networks; integrated energy systems; multienergy district (MED); multienergy systems (MES); power system flexibility.

Manuscript received November 18, 2019; revised March 13, 2020; accepted April 13, 2020. Date of publication June 4, 2020; date of current version August 20, 2020. This work was supported in part by the European Commission through the "ADDRESS," "COOPERaTE," and "DIMMER" Projects under Project FP7 207643, Project FP7 600063, and Project FP7 609084; in part by the U.K. Engineering and Physical Sciences Research Council (EPSRC) through the "MY-STORE" and "TERSE" Projects under Project EP/N001974/1 and Project EP/R030294/1; and in part by the Office of Gas and Electricity Markets (Ofgem) and Electricity North West Limited (ENWL) through the "C2C" and "Smart Street" Projects. *(Corresponding author: Eduardo Alejandro Martínez Ceseña.)*

Eduardo Alejandro Martínez Ceseña is with the Department of Electrical and Electronic Engineering (EEE), The University of Manchester (UoM), Manchester M13 9PL, U.K. (e-mail: alex.martinezcesena@manchester.ac.uk).

Emmanouil Loukarakis was with The University of Manchester (UoM), Manchester M13 9PL, U.K. He is now with Levelise Ltd., Oxford OX4 4GB, U.K. (e-mail: e.loukarakis@outlook.com).

Nicholas Good was with The University of Manchester (UoM), Manchester M13 9PL, U.K. He is now with Upside Energy Ltd., Manchester M1 1DF, U.K. (e-mail: nick.good@upside.energy).

Pierluigi Mancarella is with the Department of Electrical and Electronic Engineering, The University of Melbourne, Melbourne, VIC 3010, Australia, and also with The University of Manchester, Manchester M13 9PL, U.K. (e-mail: pierluigi.mancarella@unimelb.edu.au).

Digital Object Identifier 10.1109/JPROC.2020.2989382

I. INTRODUCTION

Historically, the energy sector has been planned, developed, and operated as a group of decoupled systems

that supply electricity, gas, and other energy vectors to end-users. The multienergy system (MES) concept challenges that idea by recognizing that what end-users actually require are services (e.g., lighting and heating), and these may be provided through multiple systems and various combinations of energy vectors (e.g., integrated electricity–heat–gas systems) [1]–[3]. By taking this approach, the MES concept offers flexibility to access a wide pool of options from multiple energy vectors and sectors to provide end-user services [4]. Some examples of use cases include reducing energy costs through the use of the cheapest combinations of energy vectors at different times [2], storing surplus renewables as heat/hydrogen [5]–[7], and switching to different vectors as a means to provide energy and network services [8]. However, modeling and assessing such flexibility is a grand challenge, especially when looking at distributed MES [9] that require integration of already complex models of different distributed energy resources (DERs), energy vectors and networks, and other key assets such as buildings [10], [11].

A special and extremely relevant and widespread case of distributed MES with huge flexibility potential are multienergy districts (MEDs). In MEDs, buildings and local DER are linked with each other through integrated, multienergy networks (e.g., for electricity and gas distribution and for district heating), and their operation in aggregate is intelligently coordinated and optimized to achieve suitable common objectives, for example, energy cost minimization or profit maximization. Buildings, where most DERs are also installed, represent an important source of flexibility [3], [12]. However, while building-level flexibility may be limited by the building's energy demands, MEDs that aggregate several buildings and DER can feature significantly greater flexibility potential [4], [13]. In fact, MEDs benefit from resource diversity and flexibility opportunities across space (e.g., from building to building), energy network/vector (e.g., from electricity to heat), and time (e.g., by energy storage): for example, by allowing multivector exchanges between buildings that take surplus electricity generation [e.g., from photovoltaics (PV)] from one building and store it as a different vector in another building, for example, using electric heat pumps (EHPs) and thermal energy storage (TES) [14], [15]. However, MED's greater flexibility also comes with greater complexity, as the buildings exchange energy through the district multienergy networks [16], [17], which needs to be modeled.

On the above premises, this article gives a comprehensive tutorial-like overview of state-of-the-art concepts and models, and presents relevant applications,[1] aimed at deploying and optimizing the flexibility value of MEDs in providing various services to the district's end-users and the wider energy system. Contents of particular relevance include.

1) Mixed integer linear programming (MILP) formulations for two-stage stochastic optimization of building and DER set-points considering relevant operational uncertainties.
2) Nonlinear mathematical models to simulate with high fidelity integrated electricity–heat–gas networks that connect buildings and DER within an MED.
3) An algorithmic approach that soft-couples the above operational optimization and network models: the resulting unified framework also represents the basis for a practical network-constrained MED energy management tool.
4) Several use cases, from different international projects and real applications, of MED flexibility for provision of multiple services internally and externally to the district.
5) Illustrative examples and case studies throughout this article, based on The University of Manchester (UoM) MED test case: this may also be used as a testbed for future multienergy network research (see the Appendix).

The rest of the article is organized as follows. Section II highlights the features of general (distributed) MES and their flexibility, with focus on buildings and DERs in districts, and provides a general MILP formulation for resource set-point optimization in the case of uncertainty. Section III introduces a nonlinear formulation for integrated electricity–heat–gas network simulation. Section IV brings together the above resource-level MILP optimization and nonlinear integrated network models into a practical tool purpose-built for MED operational optimization and active network management. Section V presents several applications of MED flexibility for the provision of multiple services for end-users and the wider energy system, including discussing potential synergies and conflicts across services. Section VI finally provides a discussion on possible research directions, applications, and challenges, while the Appendix summarizes all the information of The UoM MED test case.

II. MES, FLEXIBILITY, AND DISTRICT'S DER AND BUILDING OPERATIONAL OPTIMIZATION

This section overviews the concept of MES (compared to decoupled energy systems) and operational flexibility for MEDs. Multienergy flexibility, in particular, arises as an extension of demand side flexibility enabled by combinations of different energy vectors. An MILP-based two-stage stochastic formulation is presented to optimize the time-ahead operation of the district's multienergy resources (buildings and DER) considering uncertainty. Furthermore, as a too general MES representation of buildings may be unsuitable to capture their flexibility, specific building models are also introduced.

[1]Our studies will focus on the techno–economic modeling and complexity of the services associated with network-constrained MEDs. Further issues, such as asset ownership, contractual and market arrangements, information access, distributed optimization, and privacy, are outside the scope of this article. However, some of these are briefly discussed in Section VI.

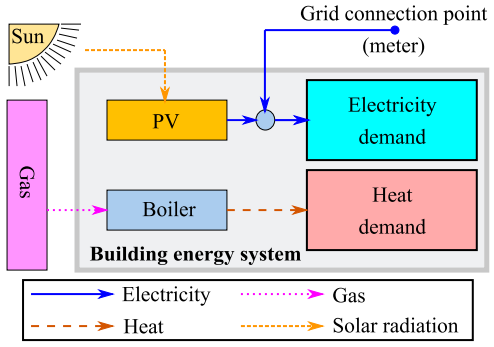

Fig. 1. *Illustrative building-level decoupled energy system.*

A. Decoupled Energy Systems and MES

Historically, end-users meet their energy demand via different energy vectors that are treated separately. For example, in Fig. 1, a building's electricity demand is met with supply from the grid and PV generation, whereas a different system is used to meet its heat demand. When considering the affordability and sustainability[2] criteria of this building's energy system, relevant costs, and emissions clearly depend on gas and electricity prices and carbon contents. End-users could reduce them by investing in more efficient devices [13]; however, the building would still have little supply flexibility.

Let us now apply the MES concept. Note that in the example from Fig. 1 the required end-use is heating, and gas is only procured as a means to provide such service.[3] Other heating options could be used, for example, combined heat and power (CHP) and district heating. The rationale for using these options is the flexibility to use the most cost-effective (least carbon intensive) combinations of solutions available from different vectors and sectors [20].[4] In the example from Fig. 2, the addition of CHP offers new options to manage energy imports and exports. However, this increases system complexity (e.g., effective CHP use may require storing surplus heat in TES) and calls for suitable techno–economic modeling, as will be shown below.

B. Demand Side Flexibility

Power system flexibility in traditionally decoupled energy systems can be enhanced by demand side management (DSM) and demand side response (DSR). DSM and DSR flexibility may also be further enhanced in the context of MES [21]. To illustrate this idea, we will elaborate on the characteristics of DSM and DSR applied to both decoupled systems and MES.

First, let us clarify the differences between DSM and DSR. DSM generally relies on motivating investments in energy efficiency (e.g., better building insulation and more efficient heating) and changes in the behavior of end-users (i.e., energy consumption) by exposing them to predefined and static signals [22]. An example is the U.K. "economy seven" tariff [23], which normally offers lower electricity prices between midnight and 7:00 h to incentivize end-users to shift their consumption (e.g., laundry and dishwashing) to this off-peak period. The mechanism is relatively straightforward to implement as it does not require any major investment in information and communications technologies (ICT) or automation. However, the flexibility captured by this mechanism can be limited as not all end-users will respond to the signal, and some could potentially experience discomfort [24], [25]. Also, the static nature of predefined price signals makes DSM inadequate to provide power system flexibility services that are actively required to balance intermittent renewable generation, alleviate network stress, etc., that is, in response to specific incumbent conditions. Such DSR can thus be considered a more advanced and effective, although potentially more expensive, version of DSM which requires the use of ICT and automation to actively deploy flexibility from DER and various building appliances [26], [27] to respond to close to real-time signals.

In the context of decoupled systems, potential end-user discomfort caused by DSR (e.g., demand curtailment [25]) could be mitigated or avoided with battery energy storage (BES) [12], [28]. However, at present, BES may still be too expensive for small domestic and commercial customers, as highlighted by the "ADDRESS" project [29], [30], which demonstrated that small end-users who partake in DSR were unlikely to have DER and might experience relatively high discomfort. End-user flexibility should then be limited to services that are called infrequently (e.g., a few times a year), but provide high payoffs, for example, network capacity support [25].

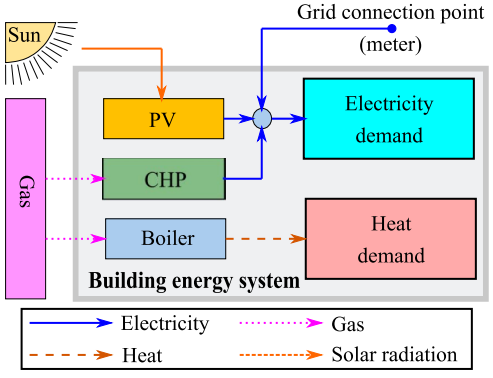

Fig. 2. *Illustrative building-level MES.*

[2]These are two pillars of the more general "energy trilemma" (and "energy quadrilemma"), which also include reliability (and social aspects) [18], [19].

[3]It should be noted that heat can also be considered as an energy vector, especially in the presence of a district heating network.

[4]There might also be additional reliability benefits in the case of electricity supply disruption, noting that in Fig. 2 electricity could also be generated by the CHP. However, this depends on the specific MES scheme.

In the context of MES, a wider variety of DER and energy vectors become available to provide DSM and DSR through multienergy flexibility. For example, TES and storage in the fabric of buildings could be used as alternatives to BES [31]. This multienergy optionality offers more cost-effective alternatives to increase end-user flexibility and reduces their risk of discomfort.[5] However, this is not free either, as the already complex models used to plan and operate different systems must now be brought together, thus motivating vast research, in the last years, in MES mathematical modeling.

C. General MES Modeling

A wide range of mathematical formulations have been developed to model MES and their capabilities to provide flexibility in the context of planning and operation applications [10], [32], [33]. The main MES modeling applications are discussed in Section III-A. The most common, general-purpose MES mathematical formulation is arguably the energy hub framework [34]. Based on this approach, all MES resources can be aggregated to form an "energy hub." This approach treats the MES and its internal components as black boxes with the aim of reducing complexity, allowing the modeling to focus on the relationships between inputs (e.g., energy vectors) and outputs (e.g., energy vectors or services). An energy hub's synthetic formulation is [35], [36]:

$$\mathbf{v}^{\mathbf{Outputs}} = \mathbf{v}^{\mathbf{Inputs}}\mathbf{C} \tag{1}$$

where $\mathbf{v}^{\mathbf{Inputs}}$ and $\mathbf{v}^{\mathbf{Outputs}}$ are arrays of energy vectors and services representing the inputs and outputs of the energy hub, respectively, and $\mathbf{C}$ is an efficiency matrix used to calculate outputs as a function of combination of inputs.

The widespread use of the energy hub model can be attributed to its simplicity and general nature, which has incentivized its use to model different types of MES, from buildings to districts and multidistrict settings (i.e., cities) [37]–[40]. However, by aggregating all resources within one MES, the energy hub approach may inherently overlook the physical characteristics of the system under consideration. For example, the thermal inertia of individual buildings and operation (set-points) of individual DER might not be adequately captured. When aggregating all buildings and DER within an MED, the energy hub approach also neglects internal multivector exchanges (through internal networks within the MED [3], [8], which will be further discussed later). Regulatory and commercial issues associated with different stakeholders within a district or across multiple districts (e.g., network operators) may also eventually be oversimplified.

[5]Thermal discomfort may occur as a knock-on effect of flexibility deployment from virtual storage in the building fabric. However, this can be actively managed and controlled based on the user's requirements [12], [28].

D. Two-Stage Stochastic Optimization of Multienergy DER and Buildings in a District

The capability of modeling the set-points of individual buildings and DER is a fundamental requirement for building and district energy managers. Accordingly, in the formulation presented below[6] we explicitly model each resource as a connection point between multiple networks within an MED [41]. From a mathematical perspective, relationships (2)–(18) [31]–[33] represent an MILP-based two-stage stochastic scheduling problem for cost minimization of multiple aggregated buildings (and DERs in general) subject to operational uncertainties.

$$\min \sum_{s,b}^{N_s} \omega_s \left(\pi i_s^{\mathrm{Elec}} Pi_{b,s}^{\mathrm{Bui}} - \pi o_s^{\mathrm{Elec}} Po_{b,s}^{\mathrm{Bui}} + \pi i_s^{\mathrm{Gas}} Gi_{b,s}^{\mathrm{Bui}}\right) \Delta t \tag{2}$$

$$\text{s.t. } Pi_{b,s}^{\mathrm{Bui}} - Po_{b,s}^{\mathrm{Bui}} = \mathrm{PD}_{b,s}^{\mathrm{Bui}} - Po_{b,s}^{\mathrm{CHP}} + Pi_{b,s}^{\mathrm{EHP}} + Pi_{s,b}^{\mathrm{BES}} - Po_{s,b}^{\mathrm{BES}} \tag{3}$$

$$Hi_{b,s}^{\mathrm{Bui}} - Ho_{b,s}^{\mathrm{Bui}} \leq \mathrm{HD}_{b,s}^{\mathrm{Bui}} - Ho_{b,s}^{\mathrm{Boiler}} - Ho_{b,s}^{\mathrm{CHP}} - Ho_{b,s}^{\mathrm{EHP}} + Hi_{b,s}^{\mathrm{TES}-} - Ho_{s,b}^{\mathrm{TES}+} \tag{4}$$

$$Gi_{b,s}^{\mathrm{Bui}} = \mathrm{GD}_{b,s}^{\mathrm{Bui}} + Gi_{b,s}^{\mathrm{CHP}} + Gi_{b,s}^{\mathrm{Boiler}} \tag{5}$$

$$Po_{b,s}^{\mathrm{PV}} = \eta e_{b,s}^{\mathrm{PV}} Po_{b,s}^{\mathrm{Solar}} \tag{6}$$

$$Ho_{b,s}^{\mathrm{EHP}} = Pi_{b,s}^{\mathrm{EHP}} \eta eh_{b,s}^{\mathrm{EHP}} \tag{7}$$

$$Hn_b^{\mathrm{EHP}} \leq Ho_{s,b}^{\mathrm{EHP}} \leq Hx_b^{\mathrm{EHP}} \tag{8}$$

$$\rho_b^{\mathrm{CHP}} \Delta t \leq Po_{b,s}^{\mathrm{CHP}} - Po_{b,s-1}^{\mathrm{CHP}} \leq \rho_b^{\mathrm{CHP}} \Delta t \tag{9}$$

$$Po_{b,s}^{\mathrm{CHP}} = Gi_{b,s}^{\mathrm{CHP}} \eta ge1_b^{\mathrm{CHP}} + \eta ge2_b^{\mathrm{CHP}} \beta_{b,s}^{\mathrm{CHP}} \tag{10}$$

$$Ho_{b,s}^{\mathrm{CHP}} = Gi_{b,s}^{\mathrm{CHP}} \eta gh1_b^{\mathrm{CHP}} + \eta gh2_b^{\mathrm{CHP}} \beta_{b,s}^{\mathrm{CHP}} \tag{11}$$

$$\beta_{b,s}^{\mathrm{CHP}} Pn_b^{\mathrm{CHP}} \leq Po_{b,s}^{\mathrm{CHP}} \leq \beta_{b,s}^{\mathrm{CHP}} Px_b^{\mathrm{CHP}} \tag{12}$$

$$Ho_{b,s}^{\mathrm{Boiler}} = \eta gh_b^{\mathrm{Boiler}} Gi_{b,s}^{\mathrm{Boiler}} \tag{13}$$

$$Hn_b^{\mathrm{Boiler}} \leq Ho_{b,s}^{\mathrm{Boiler}} \leq Hx_b^{\mathrm{Boiler}} \tag{14}$$

$$Ee_{b,s+1}^{\mathrm{BES}} = Ee_{b,s}^{\mathrm{BES}} + \left(Pi_{b,s}^{\mathrm{BES}} \eta e1_b^{\mathrm{BES}} - Po_{b,s}^{\mathrm{BES}} \eta e2_b^{\mathrm{BES}}\right) \Delta t \tag{15}$$

$$En_{b,s}^{\mathrm{BES}} \leq Ee_{b,s}^{\mathrm{BES}} \leq Ex_{b,s}^{\mathrm{BES}} \tag{16}$$

$$Eh_{b,s+1}^{\mathrm{TES}} = Eh_{b,s}^{\mathrm{TES}} + \left(Hi_{b,s}^{\mathrm{TES}} \eta h1_b^{\mathrm{TES}} - Ho_{b,s}^{\mathrm{TES}} \eta h2_b^{\mathrm{TES}}\right) \Delta t \tag{17}$$

$$En_{b,s}^{\mathrm{TES}} \leq Eh_{b,s}^{\mathrm{TES}} \leq Ex_{b,s}^{\mathrm{TES}}. \tag{18}$$

In the above formulation, πi and πo denote input (import) and output (export) prices, Pi, Hi, and Gi, respectively, represent power (electricity), heat, and gas inputs (imports) [kW], Po and Ho, respectively, denote power and heat outputs (export) [kW], PD, HD, and GD, respectively, denote power, heat, and gas demand [kW], Ee and Eh, respectively, denote electrical and

[6]In the same way as the energy hub model, the formulation provided may also be adjusted for different aggregation levels such as to represent, e.g., MEDs within a city (by replacing the superscript Bui, which currently denotes buildings). However, this approach, which centers on devices and resources rather than hubs, explicitly models the different active components within an MED (e.g., DERs and buildings with active deployment of thermal inertia), which is the key point in assessing and deploying multienergy flexibility.

thermal energy [kWh], Pn, Hn, and En, respectively, denote minimum power and heat [kW], and energy [kWh] output, Px, Hx, and Ex, respectively, denote maximum power and heat [kW], and energy [kWh] output; Δt is the length of a time period [h], ρ denotes ramping constraints [kW/h], ω_s is the probability of occurrence of a time period (further details about the stochastic formulation are provided below), β denotes binary variables [0,1], ηe, ηh, ηeh, ηgh, and ηge, respectively, denote electrical, thermal, electricity-to-heat, gas-to-heat, and gas-to-electricity efficiencies (or efficiency functions) [%], respectively.

The mathematical modeling (2)–(18) takes costs minimization from electricity and gas imports, also considering benefits from selling electricity, as the relevant objective function (2). Electricity, heat, and gas balance for every MES is modeled with (3)–(5). PV generation is modeled with (6). The set-points and limits of individual EHP units are modeled with (7) and (8), respectively. The set-points of every CHP is modeled with (9) and (11), and their capacity is modeled with (12). Equations (13) and (14) are, respectively, used to model the set-points and capacities of the boilers. The operation of the BES is modeled with (15) and (16), whereas TES operation is modeled with (17) and (18).

A superscript-based nomenclature is also used, in which the superscripts Elec, Gas, PV, Solar, CHP, EHP, BES, TES, Boiler, and Bui denote parameters associated with electricity, gas, PV, solar radiation, CHP, EHP, BES, TES, boilers, and buildings, respectively. The superscript Bui may also be modified to represent other types of DER or resource (e.g., a centralized EHP or CHP production scheme within an MED). The subscript b represents the building's number. The superscript s represents time periods. In this respect, the model addresses uncertainty by linking different time periods across scenarios which are denoted by the sequence used by the model to go through the different time periods. The approach, that is explained in detail in [33], is based on linked list [42] and is equivalent to introducing nonanticipativity constraints in multistage optimization but with significantly fewer variables. This allows the model to emulate robust constraints that depict worst case conditions [33], [43], [44], and flexibility constraints formulated as decision trees [33], [45].

E. Multienergy Flexibility Illustrative Example

The mathematical formulation provided, initially developed in the "COOPERaTE" project [46], allows addressing the limitations of decoupled systems and highlights the flexibility that can be deployed from MES. This can be illustrated, for the case of an individual building, through the systems depicted in Figs. 1 and 2. These are optimized for a typical winter weekday (24 h) considering the flat and time of use (ToU) price signals presented in Fig. 3. The latter would incentivize the systems to reduce energy consumption during the peak period (16:00–18:00 h). The

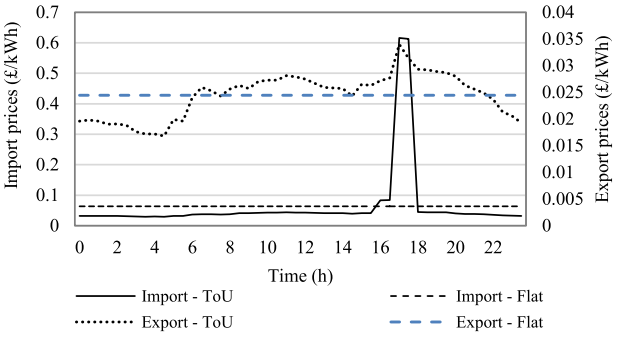

Fig. 3. *Price signals for import/export electricity considered in this article.*

prices are based on the U.K.'s context, and include a price spike associated with a signal for transmission network support ("triad mechanism") [47], [48]. The electricity profiles were taken from the Beyer building using The UoM building management system [49]. The Beyer building is one of the 26 buildings in the "Oxford Road corridor" within The UoM MED used as testbed throughout this article (see the Appendix). For illustrative purposes, and following the configuration in Fig. 2, a 20-kW (electric) CHP with an electric efficiency of 35% and a thermal efficiency of 45% is assumed to be connected to the building.

The net power inputs ($Pi^{\text{Bui}}_{b,s} - Po^{\text{Bui}}_{b,s}$ and $Hi^{\text{Bui}}_{b,s} - Ho^{\text{Bui}}_{b,s}$) of both multienergy and decoupled systems when exposed to flat and ToU prices are presented in Figs. 4 and 5, respectively. The building's manager is modeled as price taker, and the predefined system prices are assumed to be taken from relevant markets (e.g., day-ahead). As is assumed that the building of Fig. 1 does not have any DSR flexibility, in the case of decoupled system the net energy flows in Figs. 4 and 5 remain unchanged regardless of the price signals. In contrast, the MES of Fig. 2 deploys its flexibility to adjust its energy use in response to the price signals. When exposed to flat prices, in fact, CHP utilization is maximized throughout the day, as it offers cheaper

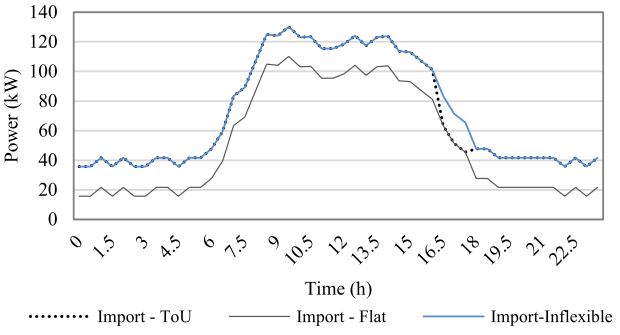

Fig. 4. *Electricity imports from "inflexible," decoupled system (same curve for both prices) and flexible MES, for both flat and ToU pricing.*

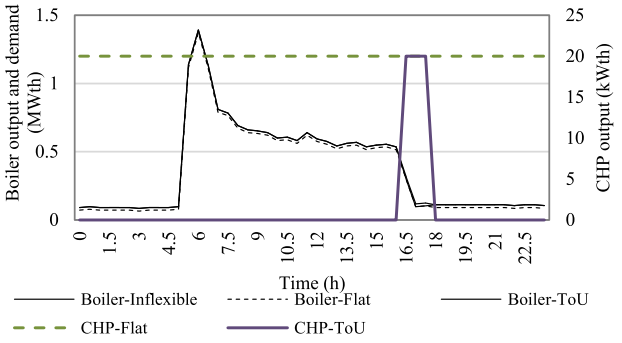

Fig. 5. ***Boiler and CHP thermal outputs for "inflexible," decoupled system (same curve for both prices) and flexible MES, for both flat and ToU pricing.***

electricity than the power grid. On the contrary, with ToU pricing, electricity prices are low during most of the day, when power is imported from the grid. In this case, then, the CHP is only used to respond to the triad price spike. This corresponds to a decrease in electricity consumption between 16:00 and 18:00 h in Fig. 4 (Import—ToU curve).

F. Building-Level MES and Virtual Storage

The formulation (2)–(18) used in the previous example explicitly models DER operation, as discussed, but still it does not capture specific multienergy flexibility features of a building (e.g., its thermal inertia).

The starting point to model such building-level flexibility is to understand its energy demand profiles, for example, from historical data from the building management system [49]. However, alternative approaches to build such profiles may be needed if the information is not available or for future scenarios. Initial high-resolution demand models focused on electricity demand [50], and were later extended to include a more comprehensive list of appliances and activities, but without consideration of occupancy-driven demand coincidence within the building [51]. This then led the authors to developing a bottom-up probabilistic tool for mapping multienergy demand profiles considering different appliances, space heating, cooking, and so on.[52]. The use of these models has become the norm during the last few years [53], [54].

Another aspect that is relevant for building modeling is their thermal inertia from the building's fabric, which can potentially be used as a form of virtual storage. This feature, which can be captured with electro-thermal models of buildings [12], [52], leads to the formulation of additional constraints that can be included in an MILP model. That is, the general multienergy mathematical formulation of MED resources presented above can be extended to address the thermal inertia characteristics of buildings and their interaction with TES. This can be carried out by adopting thermal high-resolution profiles and replacing the thermal model (17) and (18) with (19)–(23) [31]. The temperature of the building, considering outdoor temperatures, devices, and occupation (e.g., temperature gain from opened windows, and adjustments of thermostat) are modeled with (19). Occupation (represented with a binary variable β) is modeled with (20) and (21), whereas TES operation and limits are modeled with (22) and (23), respectively

$$T^{\mathrm{Bui}}_{b,s+1} = T^{\mathrm{Bui}}_{b,s} + \left(\mathrm{HD}^{\mathrm{Bui}}_{b,s} + \left(1-\alpha^{\mathrm{Bui}}_{b,s}\right)\mathrm{HL}^{\mathrm{Bui}}_{b,s} + Eh^{\mathrm{Bui}}_{b,s}/\Delta t - \left(T^{\mathrm{Bui}}_{b,s} - T^{\mathrm{Out}}_{s}\right)/\mathrm{Rh}^{\mathrm{Bui}}_{b}\right)\Delta t/\mathrm{Ch}^{\mathrm{Bui}}_{b} \quad (19)$$

$$\beta^{\mathrm{Bui}}_{b,s} \times T^{\mathrm{Bui}}_{b,s} \le \beta^{\mathrm{Bui}}_{b,s}\left(T\mathrm{set}^{\mathrm{Bui}}_{b,s} + \delta x^{\mathrm{Bui}}_{b}\right) \quad (20)$$

$$\beta^{\mathrm{Bui}}_{b,s}\left(T\mathrm{set}^{\mathrm{Bui}}_{s,b} + \delta n^{\mathrm{Bui}}_{b}\right) \le \beta^{\mathrm{Bui}}_{b,s} T^{\mathrm{Bui}}_{b,s} \quad (21)$$

$$Eh^{\mathrm{Bui}}_{s,b} = \left(\frac{Eh^{\mathrm{TES}}_{b,s}}{\mathrm{Ch}^{\mathrm{Bui}}_{b}} - T^{\mathrm{Bui}}_{b,s}\right) \times \frac{1}{\mathrm{Rh}^{\mathrm{Bui}}_{b}}\left(Tn^{\mathrm{TES}}_{b} - T^{\mathrm{Bui}}_{b,s}\right)\mathrm{Ch}^{\mathrm{Bui}}_{b} \le Eh^{\mathrm{TES}}_{b,s} \le \left(Tx^{\mathrm{TES}}_{b} - T^{\mathrm{Bui}}_{b,s}\right)\mathrm{Ch}^{\mathrm{Bui}}_{b}. \quad (22)\text{–}(23)$$

In the above relations: T denotes temperatures (°C), with $T\mathrm{set}$, Tn, and Tx representing set, minimum, and maximum temperatures (°C), respectively; HL is power loss (kW); α represents thermal gain (%); Eh denotes heat energy (kWh); Rh and Ch are, respectively, thermal resistance (°C/kW) and capacitance (kWh/°C) of the building's first-order thermal model; δn and δx are minimum and maximum temperature set-point variations (°C). In addition, as before, HD is the heat demand (kW), Δt is the length of a time period [h], β denotes binary variables, and the subscripts b and s, respectively, denote buildings and time periods; uncertainty can once again be considered by linking the time periods across scenarios [33], [42]. The simplified superscript-based notation is once again used. The superscripts Bui, Out, and TES denote parameters associated with buildings, outdoor, and TES. By modeling the buildings' thermal inertia, this formulation can thus capture additional virtual (thermal) storage.

III. INTEGRATED MULTIENERGY NETWORKS

The MES mathematical model outlined in Section II can represent both individual buildings as well as aggregates of several buildings and DER within an MED. Multiple buildings could thus be coupled together to maximize flexibility from diversity in multienergy needs and resources, for example, surplus energy from one building could be used to supply end-users within the district or be stored in other buildings. However, in practice, the MED model also requires consideration of the networks than can enable or constrain multivector exchanges. Without modeling of the linking infrastructure, in fact, the MED model may recommend operational set-points that are not technically feasible once the network limits are factored in. Also, by capturing the networks' physical characteristics, new sources of flexibility may be identified (e.g., using some network as an additional source of virtual storage).

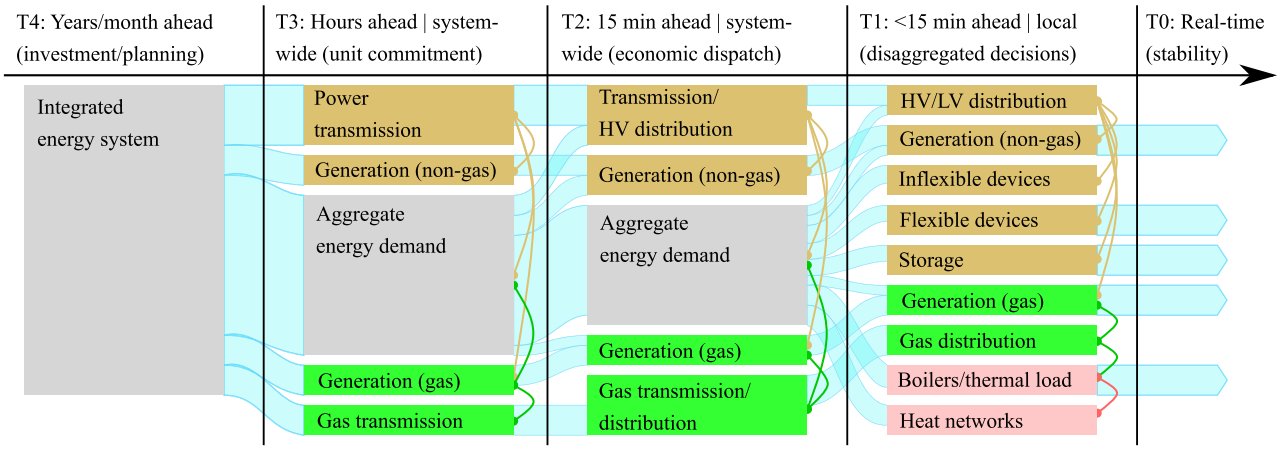

Fig. 6. ***Schematic of integrated energy systems modeling aspects over time for energy management purposes.***

On this basis, this section presents a formulation for an integrated electricity–heat–gas network model for potential applications and requirements of MEDs. Besides capturing the network's technical limitations when optimizing DER and building operation, potential benefits from flexibility embedded in the integrated network are also demonstrated, specifically, by using the heat network as virtual storage.

A. Multienergy Network Modeling Scope and Applications

The natural multivector exchanges introduced by the integration of multienergy resources within an MED can impact different networks, for which it is critical to use proper modeling. The selection of the network model should be based on the specific application under consideration, as there are multiple options ranging from simplified linear network models to detailed mathematical formulations of the steady-state or dynamic conditions of the networks.

A high-level description of different modeling applications and their time scales is presented in Fig. 6.[7] Even though these are primarily based on the structure of power systems, the main applications, from long-term investment planning (T_4) to real-time operation (T_0), are also relevant to other energy vectors and sectors, as well as, in particular, MEDs [55].

In the figure, each of the five different time scales includes one or more blocks which represent a type of constraints. Some constraints are linked with each other by lines to indicate coupling between them; for example, electricity network constraints (e.g., thermal and voltage issues) are linked to electricity generation (gas- and nongas-based) and demand. The level of detail associated with the models at each time scale are represented with the number of blocks, with aggregated models represented as single blocks, and more complex models as multiple blocks with interlinks. That is, given the high uncertainty at the planning time scales (T_4), aggregate, more abstract models may be used; on the contrary, for applications closer to real time, the aggregate demand block is replaced by a more detailed modeling of electrical network, local small-scale generation, and individual electrical devices. The use of system flexibility discussed in Section II is directly relevant for system operation and short-term operational planning (T_0–T_3). The different formulations used in these problems balance uncertainty modeling considerations and individual problems' tractability [56].

In the context of MEDs, detailed dynamic models of integrated networks could, in principle, be considered when dealing with the relatively faster timescales of Fig. 6. However, modeling the complex electricity network dynamics may not be required as relevant flexibility can still be reasonably modeled via steady-state equations even for close to real-time applications (T_0). Modeling the much slower gas network dynamics could be valuable for MES spanning large geographical areas (e.g., cities), particularly to capture the flexibility of the network to be used as a source of storage [57] and provide flexibility to, for example, support the electricity grid [58]–[60]. However, it may not be adequate to model gas dynamics in MEDs due to their relatively small geographical areas. There would also be tractability concerns associated with complex and nonlinear interactions with a potentially significant number of buildings/devices within a district. Therefore, it would appear more sensible that MEDs with their associated local electrical/gas/heat networks are represented through approximated aggregate models within T_2 and T_3, and their available controls are adjusted closer to real-time. This would happen within T_1 so that the aggregate electrical power, heat, or gas consumption matches the values determined within T_2. In a market context, penalties for deviations could also be applied to ensure coordination

[7]This diagram and the time scales (T_0–T_4) are indicative of generic applications. However, the specific characteristics would change in different countries, particularly when considering different sectors (e.g., the U.K. electricity and gas markets are balanced at different time scales [55]).

among subsequent control mechanisms. Given the need for aggregation (in T_2 and T_3) and disaggregating the decision subject to network constraints (in T_1), it is therefore assumed that there exists an entity (e.g., district operator [3]) that coordinates the operation of the devices within the MED.[8]

Based on the above, an integrated multienergy network model will be presented below. In particular, the selected network formulation can be used for both close to real-time operation (T_1) and as a basis for the aggregated modeling required for T_2 and T_3 [33]. Other modeling applications, such as investment planning (T_4), might use stronger simplifications such as linear [61], [62] or even single-node network models [32], [63] (if focus is on DER investment).

B. Multienergy Network Models

Various multienergy network models can be integrated by coupling the relevant network models using energy hub-like links [16]. An electricity–heat–gas network model will comprise, then, the models of each network as well as coupling components associated with the multienergy DER (CHP, EHP, and so on) that are connected to the different networks. However, it should be noted that this approach may not necessarily require integrated network modeling, especially for steady-state simulations when the output of the multienergy technologies is fixed, for example, when no multienergy technology is connected to a slack bus, or provide any form of response (e.g., voltage, pressure, or temperature control). This becomes evident when solving the network models, for example, by using Newton's approach, as no coupling elements appear in the Jacobian matrix [64]. In such cases, each network can be solved independently, without the need for complex integrated network models. Following the same logic, integrated models are more likely to be required in optimization rather than simulation approaches, that is, when the operation of a multienergy resource is defined through a decision variable of the optimization problem.

The electricity network model is represented with (24)–(27) [16], [17]. The connection between the network buses and a generic energy hub converter model (e.g., a building connected to the bus) is modeled with (24). The conventional power flow equations, as well as thermal and voltage limits, are modeled with (25)–(27), respectively

$$P^{\text{Elec}}_{en,s} + j\,Q^{\text{Elec}}_{en,s} = \sum_{b \epsilon en} c^{\text{Elec}}_{en,b}\left(Pi^{\text{Bui}}_{b,s} - Po^{\text{Bui}}_{b,s}\right) \tag{24}$$

$$P^{\text{Elec}}_{en,s} + j\,Q^{\text{Elec}}_{en,s} = \sum_{i} \left(Y^{\text{Elec}}_{en,em}\right)^{*} V^{\text{Elec}}_{en,s}\left(V^{\text{Elec}}_{em,s}\right)^{*} \tag{25}$$

$$\left\lceil Y^{\text{Elec}}_{en,em} V^{\text{Elec}}_{en,s} \right\rceil \leq Ix^{\text{Elec}} \tag{26}$$

$$Vn^{\text{Elec}} \leq \left|V^{\text{Elec}}_{en,s}\right| \leq Vx^{\text{Elec}} \tag{27}$$

where P and Q are, respectively, net real (kW) and reactive (kVAr) powers, $c^{\text{Elec}}_{en,b}$ is an efficiency matrix (from the energy hub approach) connecting buildings and buses, Y denotes admittances (S), V and I, respectively, denote voltages (V) and currents (A), and the superscripts en and em denote buses while l denotes a line connecting two buses (en and em). As before, Pi and Po, respectively, represent power inputs and outputs (kW), the subscript s represents time periods, and superscripts are used to denote parameters associated with the electricity network (Elec) and building (Bui) models.

For gas networks, pressure dynamics are not significant for small networks such as those within districts.[9] Accordingly, for MED applications it is convenient to model the gas network with a steady-state model such as in [67] and assume that sufficient pressure is provided by the external gas network. Similar equations are used in [68]–[71]. Following an approach similar to the one for the electricity network, then, DERs and buildings that are connected to the gas network are modeled as links between different networks or between gas network and nodal consumption, as shown in (28). The specific hydraulic equations used in this article are (29)–(30) [16], whereby (29) represents the gas injected to or extracted from a node as a nonlinear steady-state function of pressures, whereas (30) models the maximum and minimum pressures of the network

$$q^{\text{Gas}}_{gn,s} = \Delta t \sum_{b \epsilon gn} c^{\text{Gas}}_{gn,b} Gi^{\text{Bui}}_{b,s} \tag{28}$$

$$q^{\text{Gas}}_{gn,s} = \sum_{gm} \left\{ K^{\text{Gas}}_{gn,gm} \text{sign}\left(p^{\text{Gas}}_{gn,s}, p^{\text{Gas}}_{gm,s}\right) \times \sqrt[2]{\text{sign}\left(p^{\text{Gas}}_{gn,s}, p^{\text{Gas}}_{gm,s}\right)\left[\left(p^{\text{Gas}}_{gn,s}\right)^2 - \left(p^{\text{Gas}}_{gm,s}\right)^2\right]} \right\} \tag{29}$$

$$\left(pn^{\text{Gas}}\right)^2 \leq \left|\left(p^{\text{Gas}}_{gn,s}\right)^2\right| \leq \left(px^{\text{Gas}}\right)^2. \tag{30}$$

As notation, q denotes flows (in this case gas) injected to a node (m^3/h), Gi denotes gas consumption, p represents nodal pressures (Pa), K denotes the pipeline constant, pn and px are, respectively, the minimum and maximum pressure limits or flowing through a pipe [Pa], **c** is the efficiency matrix (energy hub approach) to link gas import from buildings/DERs and nodal flows,[10] and the subscripts gn and gm denote nodes. As before, a superscript-based

[8] In practice, different setups may occur, also depending on the specific business model developed—see also Section VI. These aspects also pave the way to relevant research into decentralized optimization.

[9] For a large-scale gas network, virtual storage flexibility is associated with the network's linepack, which in turn depends on its operating pressures [65]. Transient flow equations should then be used [58] and consider the minimization of compressor power as part of the objective function [66], in case. In a relatively small district operating at low or even medium pressures, however, linepack is small and its flexibility therefore limited. Additionally, there are few practical ways to actively control gas pressure within a district, while the virtual storage potential of a heat network, which depends on its thermal features, as discussed below, may be actively influenced by modulating operating temperatures and flow rates.

[10] Note that the components $c^{\text{Gas}}_{gn,b}$ of the efficiency matrix in (28) should also include factors to convert kWh to m^3/h (e.g., based on a calorific value of 39.2 MJ/kg, i.e., 1 m^3 = 11.4 kWh).

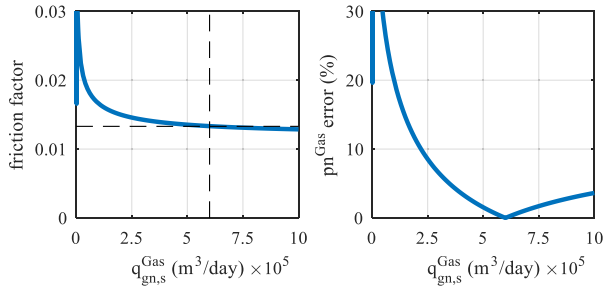

Fig. 7. *Example of (left) friction factors and (right) squared gas pressure drop error (in %) from assuming a constant friction factor (0.0133)—parameters as a function of flow.*

nomenclature is used, that is, the superscripts Gas and Bui denote parameters associated with the gas network and building models. The sign function used in (29) is equal to $+1$ when $p^{Gas}_{gn,s} > p^{Gas}_{gm,s}$ and -1 otherwise.

The pipeline constant, K, which in turn depends on the friction factor, may be calculated using different methods based on the characteristics of the network and pressures [72], [73]. However, what is typically indicated as a constant is in reality a highly nonlinear function of the flow, and different equations may apply, depending on the flow conditions and pipe characteristics [72]. This is illustrated in Fig. 7, which shows (left) the friction factor as a function of gas flow for a 1 km, 500-mm pipe, and 20 °C flow temperature. The pressure drop coefficient is a function of the friction factor and varies with the flow conditions in a nonlinear, nondifferentiable manner. The figure also shows (right) the squared gas pressure drop error assuming a fixed pressure drop coefficient value (at fully turbulent region). It should be noted that while the error in % of the exact pressure drop can be significant for low flows, its impact should be inconsequential, given that the corresponding pressure drop would be small. This poses the basis for using a constant friction factor value (and hence a pipeline constant) taken from the turbulent region as a suitable approximation. A similar reasoning may be used when modeling heat networks.

With regards to heat networks, their modeling is also coupled to the other networks through energy conversion links and is composed of a hydraulic module and a thermal module.

The hydraulic module is based on conventional steady-state equations as for the gas case.[11] Hence, the connections between the heat network and a generic energy hub (and, in particular, a building) are formulated with (31) using an efficiency matrix approach, the water nodal balance is denoted by (32), the water flow in each pipe is calculated with (33), and the pressure limits are imposed with (34) [74]–[76]

$$q^{Heat}_{hn,s} = \Delta t \sum_{b \epsilon hn} c^{Heat}_{hn,b} \left(Hi^{Bui}_{b,s} - Ho^{Bui}_{b,s} \right) / \Delta T^{Heat}_{hn,s} \tag{31}$$

$$q^{Heat}_{hn,s} = \sum_{l \in hm} ql^{Heat}_{l,s} \tag{32}$$

$$ql^{Heat}_{l,s} = K^{Heat}_{hn,hm} \text{sign}\left(p^{Heat}_{hn,s}, p^{Heat}_{hm,s} \right) \times \sqrt[2]{\text{sign}\left(p^{Heat}_{hn,s}, p^{Heat}_{hm,s} \right) \left[\left(p^{Heat}_{hn,s} \right)^2 - \left(p^{Heat}_{hm,s} \right)^2 \right]} \tag{33}$$

$$pn^{Heat} \leq p^{Heat}_{hn,s}. \tag{34}$$

In the above relations, q and ql denote flows (in this case water), respectively, injected to a node and flowing through a pipe (m^3/h), $c^{Heat}_{hn,b}$ are again efficiency matrix components (energy hub approach) to link heat import from buildings and nodal flows,[12] ΔT represents temperature drops (°C), K is the pipe constant, p and pn are pressure and minimum pressure limits (Pa), the subscripts hn and hm denote nodes, and the superscript Heat parameters associated with the heat network.

In addition to the hydraulics, a thermal module that models temperatures across the heat network is also needed. In fact, given that energy roughly travels with the flow speed of water, depending on the size of the network, there might be significant delays to propagation of supply temperature variations. While for limited-length networks temperatures may be derived through steady-state exponential functions of flow [16], [77], for larger networks such a representation would not be sufficient. Furthermore, this would also neglect any virtual energy storage potential of the network itself, while the energy contained in the network's water, and therefore its thermal capacity, may not be negligible even for relatively small sizes.[13] The heat network temperature dynamics are also modeled here through the set (35)–(39) [78]–[80], where it is assumed that supply temperatures and flows remain constant throughout an optimization time step. More specifically, the temperature drop across a device, and considering previous temperatures, is modeled with (35). The temperature drop across a heat exchanger is modeled with (36). The pipe temperature dynamics, also considering the effects of the mass flow rate and ambient temperatures, are modeled with (37) and (38). The nodal temperature balance is described as follows:

$$\Delta T^{Heat}_{hn,s} = \int_{\tau=(s-1)\Delta\tau}^{s \times \Delta\tau} \left(T^{Heat}_{hn,s,\tau} - Td^{Heat}_{hn,s,\tau} \right) d\tau \tag{35}$$

$$T^{Heat}_{hn,s,\tau} = \left(Td^{Heat}_{hn,s,\tau} - T^{Out}_{s} \right) \exp\left(\frac{-h^{Heat}_{hn}}{q^{Heat}_{hn,s} w} \right) + T^{Out}_{s} \tag{36}$$

[11] These equations are deemed adequate to describe the heat network's hydraulics considering that pressure dynamics travel with the speed of sound and assuming that the fluid is incompressible.

[12] The heat capacity of water is taken as 4.182 kJ/(kg·°C).

[13] Differently from gas networks, as discussed earlier.

$$m_{l,s}^{\text{Heat}} w \frac{\partial Tl_{l,x,\tau}^{\text{Heat}}}{\partial \tau} = ql_{l,s}^{\text{Heat}} w \frac{\partial Tl_{l,x,\tau}^{\text{Heat}}}{\partial x} - h_{hn}^{\text{Heat}} \left(Tl_{l,x,\tau}^{\text{Heat}} - T_s^{\text{Out}} \right) \quad (37)$$

$$Tl_{l,x,\tau}^{\text{Heat}} = T_{hn,s,\tau}^{\text{Heat}}, x \in \left[0, L_l^{\text{Heat}}\right] \quad (38)$$

$$Tn_{hn,s,\tau}^{\text{Heat}} \sum_{l \in hn} \text{dir}\left(ql_{l,s}^{\text{Heat}}\right) \left| q_{l,s}^{\text{Heat}} \right| = \sum_{l \in hn} \left[Tl_{l,x,\tau}^{\text{Heat}} \text{dir}\left(-ql_{l,s}^{\text{Heat}} \right) \left| q_{l,s}^{\text{Heat}} \right| \right], \quad x = L_l^{\text{Heat}}. \quad (39)$$

In the above relations, in addition to the symbols presented for the heat network's hydraulic equations, Td and Tl denote temperatures changes (°C) through time introduced by input and output flows and flows through the pipes, m is the mass of water in a pipe (m^3), w denotes heat capacity [kJ/(kg·(°C)C)], L is the pipe's length (m), and h is the heat transfer coefficient (kW/K).

C. Example of Integrated Energy Network Studies

The integrated electricity–heat–gas network model presented here was initially developed in the "DIMMER" and "MY-STORE" projects [33], [81], [82] and applied to The UoM MED test case. The networks were simulated by taking the buildings' multienergy demand as inputs, and declaring one or more DER as slack or active units (e.g., for active voltage or temperature control). The model was then solved by Newton's method, which, as explained earlier, will include elements that couple the different networks if the networks are actively integrated (e.g., a multienergy device is one of the slack generators or is used as an active unit) [64], [76]; otherwise, each model can be solved independently. In any case, it is important to note again that the networks will generally be actively coupled for optimal power flow or other forms of optimization [33]. Some example of relevant integrated network studies that were conducted is given in this section.

First of all, let us analyze the technical impacts that different DER can have on different networks of The UoM MED at peak time, assuming no DER and that only gas boilers are used for heat supply (see the Appendix). More specifically, the color-maps in Fig. 8 show: 1) voltage deviations, where white indicates nominal voltages (close to 1 pu) and darker colors indicate areas with potential low voltage issues (closer to 0.96 pu) and 2) pressure drop variations, where white indicates pressures close to 7 bar and darker colors indicate areas with low pressure issues (close to 1.5 bar). The study highlights areas where potential voltage/pressure issues may arise (thermal constraints can also be analyzed, as discussed in Section IV), which is key when sizing and placing new DER [16], analyzing the feasibility of MED operation strategies [17], and planning for network reinforcements [83].

Let us now illustrate the use of the heat network as a source of virtual energy storage flexibility [84], [85]. The UoM MED is modeled for a typical winter weekday and, as before, only gas boilers are considered to meet heat

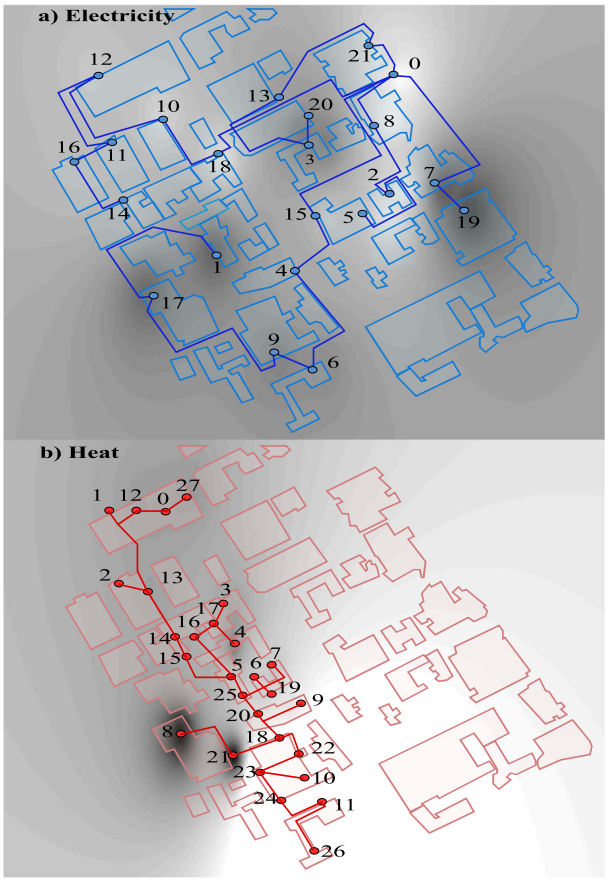

Fig. 8. *Color maps of (a) voltage deviations (electrical network) and (b) pressure drops (heat network) for the UoM MED test case at peak time.*

demand. Further virtual storage in the fabric of buildings is ignored. Under these conditions, networks are the only source of flexibility. The model is set to produce additional heating beyond heat demand (preheating) one hour before the peak period and thus reduce peak heat generation requirements thanks to the temperature dynamics of the heat network. The results are presented in Fig. 9, where some 10% of the network thermal load seen by the heat supply can be decreased owing to the heat network's virtual storage flexibility. This flexibility mainly depends on

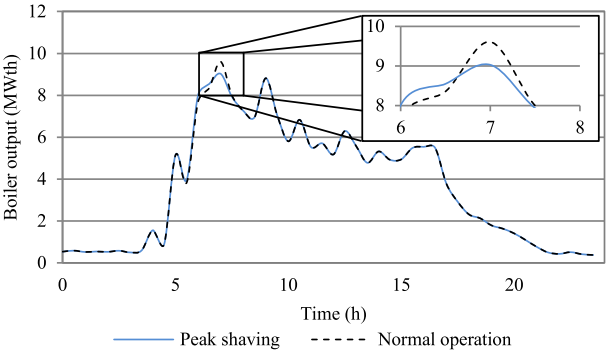

Fig. 9. *Boiler output considering normal operation and the use of heat network flexibility as a source of virtual energy storage for peak shaving.*

the size of the network (e.g., volume of water in the pipes), and can be combined with other sources of thermal storage (including more virtual storage from thermal inertia in the fabric of buildings) [86], [87].

Another important note to make here is that, as the system in this example is supplied by a gas boiler, the heat network's flexibility also affects the gas consumption of the system, reducing the gas network loading. Similarly, such virtual storage would also impact electricity consumption or network demand for other energy vectors if heat was supplied with one or more EHP, CHP unit, or other technologies. This highlights how in an MES context deploying flexibility available in one network may actually affect all involved energy vectors and networks, as widely discussed in [9].

IV. NETWORK-CONSTRAINED ENERGY MANAGEMENT OF MEDs

The multienergy resource scheduling MILP and the integrated network models presented above can be combined to create an MED energy management tool that captures the physical constraints and flexibility options from both DERs and networks. This section discusses approaches for coupling these models, presents a specific soft-coupling methodology, and illustrates the use of flexibility to relieve network constraints and actively manage the district's networks.

A. DER Scheduling and Network Model Coupling

In the context of MEDs, impacts across multiple networks will increase with higher DER integration before security limits [88], particularly as flexibility becomes a more prominent source of network capacity [33]. As a result, there has been growing interest in developing MES models that bring together optimal DER operation and multienergy network models [10], [89], with a great deal of simplification in network modeling [65], [68], [90], [91]. Other approaches that address the full complexity of the models typically deploy metaheuristics [92] or multilevel [93] optimization. The former, in particular, may be adopted by soft-coupling resource scheduling and network models. In this approach, operation is first optimized without considering the presence of the networks, and the outputs of the operation model are then used to simulate network operation and check for network limits. Although this approach may in principle limit the ability to fully exploit multienergy flexibility to actively manage network constraints, soft-coupling is a common approach to test predefined operation strategies and inform network operators about potential reinforcement needs [94], [95]. The use of soft-coupled models may actually be preferred for large-scale systems and when considering DER integration with little or no resource coordination, for example, decarbonization pathways [96]. By neglecting complexity from the coupling of DER operation and network models, this type of approaches can also focus on producing high spatial (e.g., per postcode) and temporal (half-hourly or more frequently) MES analysis over large areas [97], which is of great relevance for policy makers, regulators, and other actors interested in urban development.

A heuristic soft-coupling modeling approach is selected here that strikes an ideal tradeoff between optimality (though the MILP-based resource scheduling) and feasibility (via the detailed nonlinear network model analysis). The mathematical formulation, taken from [33], can be expressed as follows:

$$\min \Delta t \sum_{s} \omega_s \left(\pi i_s^{\text{Elec}} Pi_s^{\text{Dis}} - \pi o_s^{\text{Elec}} Po_s^{\text{Dis}} + \pi i_s^{\text{Gas}} Gi_{b,s}^{\text{Dis}} + xPF_s M\right) \tag{40}$$

$$Pi_s^{\text{Dis}} - Po_s^{\text{Dis}} = \text{LP}_s \sum_{b} \left(Pi_{b,s}^{\text{Bui}} - Po_{b,s}^{\text{Bui}}\right) \tag{41}$$

$$0 = \text{LH}_s + \sum_{b} \left(Hi_{b,s}^{\text{Bui}} - Ho_{b,s}^{\text{Bui}}\right) \tag{42}$$

$$\begin{aligned} Kf_s \geq & \sum_{ne} \sum_{b \in ne} \left[Kfd_{ne,b,s}\left(Pi_{b,s}^{\text{Bui}} - Po_{b,s}^{\text{Bui}}\right)\right] \\ & + \sum_{nh} \sum_{b \in nh} \left[Kfd_{nh,b,s}\left(Hi_{b,s}^{\text{Bui}} - Ho_{b,s}^{\text{Bui}}\right)\right] \\ & + \sum_{ng} \sum_{b \in ng} \left[Kfd_{ng,b,s} Gi_{b,s}^{\text{Bui}}\right] + Kfc_s - xPF_s. \end{aligned} \tag{43}$$

In (40)–(43) [33], πi and πo are energy prices (£/kWh), Pi^{Dis} and Po^{Dis} are district power input and outputs (kW), xPF is a feasibility constraint that allows the system to exceed network limits at a high penalty cost (M), LP and LH denote losses [kW], Kf denotes a network limit (e.g., thermal, voltage, and pressure), Kfc and Kfd provide a linear approximation of a binding network constraint (e.g., losses, loading for lines exceeding their thermal limits, and flows associated with nodes with voltage issues), and the subscripts s, b, ne, nh, ng denote time periods, buildings, electrical buses, heat nodes, and gas nodes, respectively.

The objective function of the MED (i.e., cost minimization) is modeled with (40). Equation (40) considers only costs associated with internal gas consumption (e.g., to supply gas boilers and CHP), and costs/revenue from importing/exporting electricity from/to the primary substation that feeds the whole MED (i.e., 33 to 6.6 kV).[14] The electricity balance within the district, including electricity imports and exports, and losses is modeled with (41). The heat balance within the district, including heat network losses, is modeled with (42). Heat imports and exports could also be

[14]Once again, this approach where the whole district rather than individual buildings is charged for energy consumption applies for cases where all buildings are managed/owned by a same actor. Charges per building, as previously denoted by (2), and internal market arrangements may be required if different actors own or manage the buildings [3]—see also Section VI.

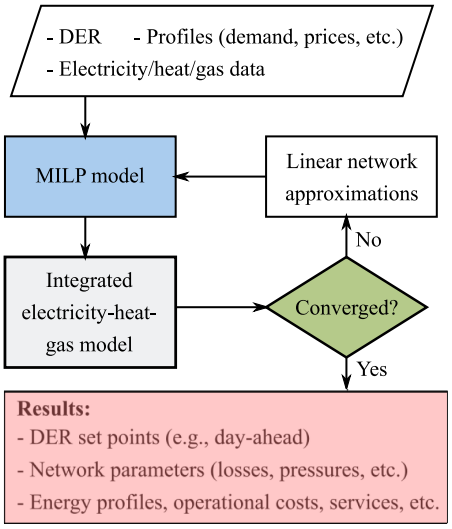

Fig. 10. *Iterative approach to soft-couple MILP-based resource scheduling and nonlinear integrated network models for MED energy management.*

included to consider large heat networks that supply multiple MEDs.

In terms of practical energy management tool implementation, the heuristic problem proposed can be solved using the soft-coupling algorithm presented and summarized in Fig. 10. Namely, the approach consists of, first, solving the MILP model with all losses and network constraints in (43) ignored. Then, the resulting DER set-points are used to simulate detailed network operation with the integrated electricity–heat–gas model, and the network impacts are assessed. Assessment of power losses and active network constraints, that is, when a limit of the network is exceeded, are then identified and modeled with (43). For that purpose, the parameters for the linear model are taken as the differentials of the binding network constraints and losses (from the integrated model) with respect to the nodal net flows.[15] These differentials provide linear approximation of the electricity, heat, and gas losses or network limits, which are modeled with Kfd and Kfc. This approach, which is similar to Newton's method, uses differential equations to formulate linear approximation of the network models at relevant operating points. This information is then passed back to the MILP model so that the operation of the DER in the MED can be revised. The process is repeated until the error (difference between set-points in two consecutive iterations) decreases below a predefined threshold. More information about modeling, developed in [81] and [98], can be found in [33].

B. Multienergy Active Network Management

The proposed network-constrained MED tool can effectively manage the DER set-points of the system to meet different targets (e.g., minimizing costs or increasing profit

[15]Note that the differentials of nonbinding constraints where the networks are operating within their limits are not modeled as their value is zero.

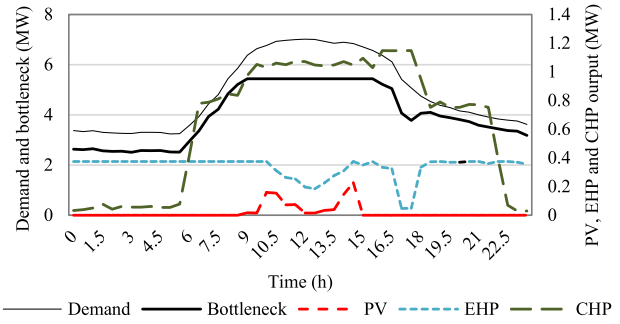

Fig. 11. *Active power flow through the most loaded line (bottleneck) and aggregated electricity demand and DER output-constrained case.*

from the trade of energy services), while also actively managing network limits. This is again demonstrated with applications to The UoM MED test case. In this example, it is assumed that a total of 60 devices as PV (3.4 MW), CHP (2.7-MW electric), EHP (2.6-MW thermal), and gas boiler (24 MW) are installed throughout the district (more information can be found in [33]). The ToU prices presented in Fig. 3 are considered. To illustrate the significance of network constraints, the thermal capacity of the electricity distribution network has been artificially reduced (additional types of constraints too are explored in [33]). The results of the study are presented in Fig. 11 (electricity vector) and Fig. 12 (heat vector). The gas profiles are not displayed as there are no bottlenecks in the gas network and no gas injection back into the network. More complex examples addressing gas network modeling can be found in [39], [57], and [65].

This article shows that the MED mainly relies on electricity imports, and the use of EHP to meet its heat demand during periods when electricity prices are low (i.e., before 6 A.M.). Afterward, as electricity prices and demand increase, operating the EHP using grid imports becomes too expensive, which motivates using CHP to meet part of the heat and electricity demand (including EHP imports), especially at 17:00 h where there is a

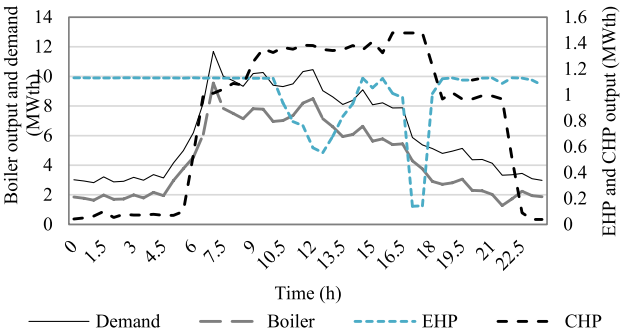

Fig. 12. *Aggregated thermal demand and DER output-constrained case.*

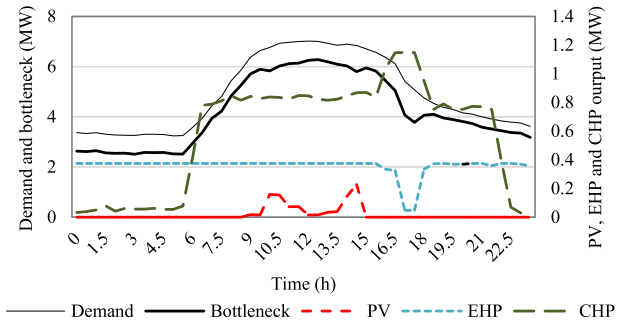

Fig. 13. ***Active power flow through the most loaded line (bottleneck) and aggregated electricity demand and DER output-unconstrained case.***

price spike. It can be seen in Fig. 11 that the bottleneck line, which has a 5.4-MW capacity in this example (line 12 connecting buses 0 and 15, see the Appendix) [33], becomes overloaded between 9:00 and 15:00 h.

To relieve the line constraint during this time, the MED can actively manage the set-points of the CHP, boilers, and EHP. The resulting operational strategy can be appreciated by comparing the results from Figs. 11 and 12 (constrained case) with those from Figs. 13 and 14 (unconstrained case). In the unconstrained case, where the technical limits of the network (e.g., voltage and thermal limits) are ignored, the loading of the bottleneck line would exceed its 5.4 MW, which would make the solution unfeasible unless the electricity network is reinforced. As the line limit is neglected, the operation of the EHP and CHP is mainly based on the price signals, for example, low electricity prices between 23:00 and 5:00 h, and high prices at 17:00 h (see Fig. 3). Accordingly, CHP generation is low before 5:00 h and the device operates at maximum capacity during the peak period. The EHP mainly operates at a constant output, except during the peak time where electricity imports become more expensive.

V. MED FLEXIBILITY AND GRID SERVICES

The model proposed and illustrated in Section IV allows optimal management of the MED's flexibility by actively changing its energy flows in response to different forms of signals, namely prices and constraints. This section explores the potential use of the district's multienergy flexibility to simultaneously provide combinations of services to the electricity grid and relevant markets. It will also be shown that there may be synergies and conflicts between different services which cannot be captured when the services are assessed in isolation.

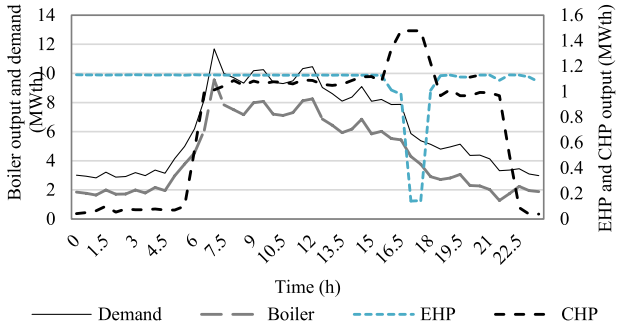

Fig. 14. ***Aggregated thermal demand and DER output-unconstrained case.***

A. Modeling Grid Services

The general formulation provided in Section IV can be applied to account for grid services that are incentivized with price signals (e.g., triad) [46], [99], [100] or require explicit network modeling such as managed connections [101] and capacity support [25], [83],[16] and reserve [106]–[108]. To illustrate this, the MED operational model presented above is further extended to consider one type of reserve service based on explicit modeling of DER available headroom, as shown in

$$R^{\mathrm{CHP}}_{b,s} \leq \sum_{b} Px^{\mathrm{CHP}}_{b} - Po^{\mathrm{CHP}}_{b,s} + \eta e^{\mathrm{BES}}_{b} \frac{Ee^{\mathrm{BES}}_{b,s} - En^{\mathrm{BES}}_{b,s}}{\Delta t} + Px^{\mathrm{EHP}}_{b}. \quad (44)$$

This is a bespoke equation for an MES comprising CHP, BES, and EHP. That is, the upward reserve that can be provided at a given time period is calculated as a function of CHP power generation headroom, available electricity that can be taken from BES, and demand that can be reduced by ramping down the EHP [8]. Alternative formulations for this equation, as well as models for other forms of reserve can be found in [8], [109], and [110].

This reserve service will be applied next in conjunction with the modeling features previously introduced.

B. Conflicts and Synergies Among Services

The potential for MEDs to provide flexibility to reduce costs for multienergy end-users [32], [111] and partake in the provision of multiple ancillary services [8], [112], [113] calls for investigating synergies and conflicts that may arise [8], [114], and the relevant impacts on the MED business case too.

To this end, let us use The UoM MED test case to study the effects of simultaneous provision of energy arbitrage, active network management, and reserve services, by simulating the following cases.

1) *Arbitrage:* The district is exposed to ToU electricity prices, which incentivize shifting electricity generation to the off-peak period (this corresponds to the studies already shown in Figs. 13 and 14).

[16]The latter applications have been explored in detail by the authors in several industrial-led research projects, e.g., "Capacity to Customers" (C_2C) [102], [103] and "Smart Street" [104] projects, which centered on active distribution network management [83], [105].

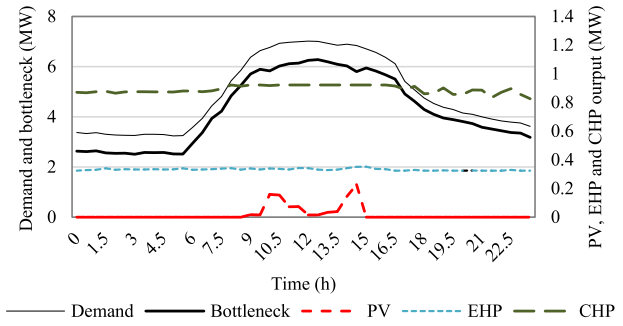

Fig. 15. *Active power flow through the most loaded line (bottleneck) and aggregated electricity demand and DER output-flat electricity prices.*

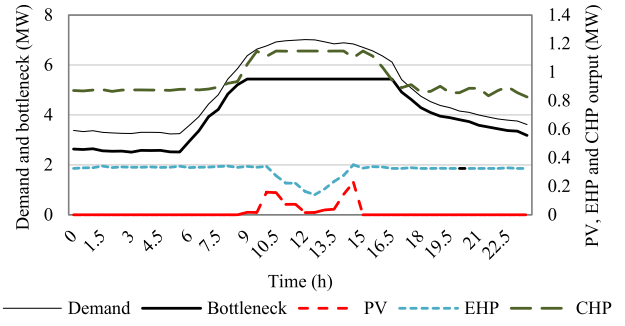

Fig. 17. *Active power flow through the most loaded line (bottleneck) and aggregated electricity demand and DER output-flat electricity prices and network constraints.*

2) *Baseline:* The district is exposed to flat electricity prices, which do not incentivize the use of flexibility (see Fig. 15).
3) *Reserve:* The district is exposed to flat electricity prices and flat upward reserve prices (see Fig. 16).
4) *Active Network Management:* The district is exposed to flat electricity prices and is subject to network constraints (see Fig. 17).
5) *All:* The district is exposed to ToU electricity and flat reserve prices, and network constraints (see Fig. 18).

The Arbitrage case where ToU prices are introduced was presented above in Figs. 13 and 14. As discussed, the MED actively changes the use of different technologies in response to the variable prices. In the Baseline case (see Fig. 15), the district MES mainly relies on the use of local CHP generation to meet its energy needs. The operation is consistent throughout the day as the prices do not change. When reserve prices are introduced (see Fig. 16), there is an incentive for the MED to increase its headroom which can be achieved through different DER uses, for example, reducing CHP generation and/or increasing EHP use, in this example. The decision to use either option, or a combination, will depend on the prices faced by the district. In the active network management case where network constraints are considered (see Fig. 17), the MED is operated to meet the technical limits of the networks (in this example associated with the thermal limits of a line). All cases of Fig. 18 clearly represent a tradeoff solution.

What is essential to note from these studies is that the expected system behavior in providing a given service fundamentally changes once other services are introduced (due to the associated conflicts and synergies). For example, the introduction of ToU incentivizes the MED to arbitrage and reduce imports during the peak time (see Figs. 13 and 14). However, when both ToU and reserve are considered (see Fig. 18), the MED does no longer arbitrage at peak times. This is not the case for the reserve service, as the MED provides similar levels of reserve when exposed to reserve prices only (see Fig. 16) and to reserve, arbitrage and active network management signals altogether (see Fig. 18). However, the operation of the district is fundamentally different in those two cases. In fact, when only exposed to reserve prices, the MED heavily relies on electricity imports to supply the EHP throughout the day (see Fig. 16). On the contrary, electricity imports are low when all services are considered, as the system relies more on the CHP to supply the EHP. The operation of the MED, in terms of energy imports and exports and provision of services, can thus change significantly when new signals (e.g., new services) are introduced. Properly modeling these effects, for example, by using the framework provided, is critical for the effective deployment and integration of MEDs in practical regulatory settings [115] and development of new planning practices [116].

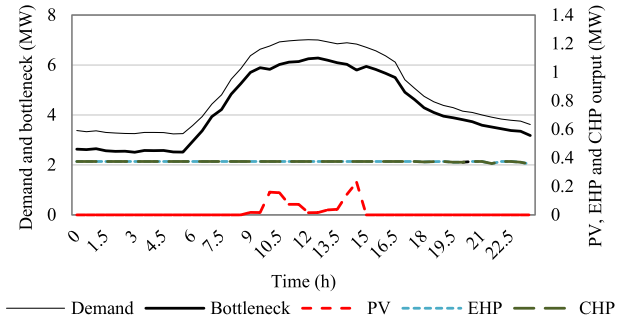

Fig. 16. *Active power flow through the most loaded line (bottleneck) and aggregated electricity demand and DER output-flat electricity prices and flat reserve prices.*

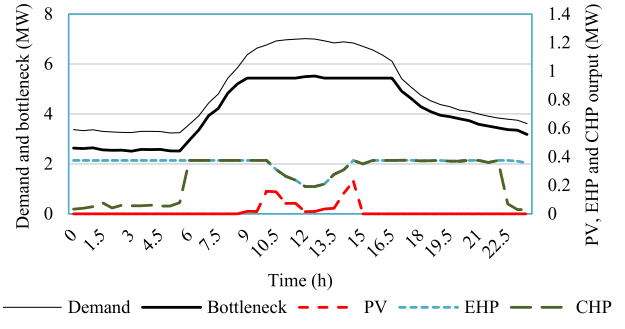

Fig. 18. *Active power flow through the most loaded line (bottleneck) and aggregated electricity demand and DER output-ToU electricity prices, flat reserve prices, and network constraints.*

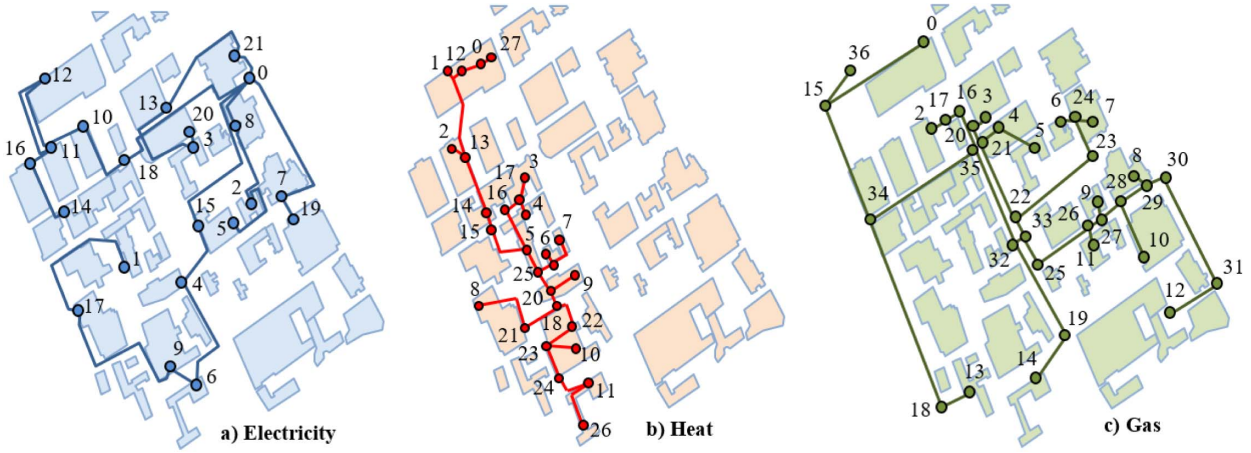

Fig. 19. *Diagram of the (a) electricity, (b) heat, and (c) gas networks within the UoM MED test case.*

VI. FUTURE RESEARCH DIRECTIONS

The framework and tools presented have already been applied in a number of real-world MES and MED applications. However, much research work is still to be done in these areas. Some potential directions are provided below.

One important topic in the general context of MES is the use of hydrogen [6], [7], [58] as an energy vector to enable the transition to very low-carbon power systems in support of or replacing electrification of heating and transport. For MEDs, one key question would also be whether entire districts or even cities could use (green) hydrogen as the central energy vector as opposed to electricity, or in any case what role it could play for urban decarbonization, and under which conditions. See, for example, a number of relevant ongoing projects [117], [118].

Regarding applications of multienergy flexibility, understanding the role and opportunities for MES in making the energy systems more reliable as well as resilient to high-impact low-probability events (e.g., natural disasters) is another important area of research, also considering that the severity and frequency of extreme events may increase in the future due to climate change [119]–[121]. For MEDs, in particular, it is crucial to be able to assess how districts may be able to provide system support, reliability, and resilience [122]. At the same time, it will be critical to properly account for the new tradeoffs that these services are introducing to the system [8], [115], particularly by reliably reducing investments in traditional network and generation capacity (e.g., reducing capacity margins).

The integration of a large number *of* DER owned and operated by different actors (e.g., aggregators, network operators, and end-users) within MEDs or across multiple districts might make traditionally centralized controls obsolete and potentially infeasible [56], [123]. New decentralized optimization algorithms might therefore be required, whereas multilevel approaches would have to be developed to account for the effects of these algorithms across multiple energy vectors and at different and potentially overlapping time scales [124]. In this regard, the different models presented in this article could be soft-coupled at different time scales by, for example: 1) deploying the MILP model (without network constraints) for MED investment planning [41]; 2) using the full network-constrained MED model for time-ahead applications [33]; and 3) using the integrated network simulator to assess network conditions at regular intervals [16] and reoptimizing the MED if required, in case in a rolling horizon fashion. However, significant research is still required to develop additional models covering intermediate and overlapping time scales, and proper off-/online feedback loops. A particular challenge would be to deal with computational complexity, which will be exacerbated with the expected large-scale DER integration. Increasing DER integration will also bring more challenges associated with impacts on local and system-level prices and performance, different DER ownership, privacy requirements, and handling of data of end-users and other stakeholders [125].

Local multienergy markets may offer a potential solution to coordinate DER operation, price the value of multienergy flexibility, and incentivize its use to support end-users and the wider energy system. New concepts, such as markets based on transactive energy approaches, may provide the above benefits while also protecting the privacy of the different actors involved in the markets [126], [127]. However, research to properly develop transactive mechanisms that would work effectively across different energy vectors and sectors is yet in its infancy (see, for instance, [109]), and poor exchange of data and signals might even result in flexibility deployment causing network issues, for example, new demand peaks, higher system stress levels, and reduced system reliability and resilience.

These challenges, and many more, will have to be tackled with fresh research to facilitate the development of affordable, sustainable, reliable, and resilient energy systems. In this respect, flexibility from MES and MEDs will be critical to deliver a low-carbon energy future. ■

Table 1 Parameters of the 6.6-kV (1-MVA base) Electricity Distribution Network Within the UoM MED

Line No.	Bus		R	X	Capacity
	From	To	(pu x 10^{-4})	(pu x 10^{-4})	(A)
1	0	18	5.1115	6.8685	540
2	18	10	2.0305	2.7285	540
3	10	12	4.1756	5.6109	540
4	12	11	2.7078	3.6386	540
5	11	16	0.6274	0.8430	540
6	16	14	2.1157	2.8430	540
7	1	17	4.1682	5.6011	540
8	17	9	4.6369	6.2309	540
9	9	6	1.3649	1.8341	540
10	6	4	3.5409	4.7580	540
11	4	15	2.4066	3.2339	540
12	0	15	5.6184	7.5497	540
13	0	8	2.0804	2.7956	540
14	8	2	2.3038	3.0957	540
15	2	5	2.5241	3.3918	540
16	0	7	4.6178	6.2052	540
17	7	19	1.0629	1.4282	540
18	0	21	1.8762	2.5212	540
19	21	13	4.0639	5.4609	540
20	13	3	4.0771	5.4787	540
21	3	20	0.6710	0.9017	540

Table 2 Parameters of the 85 °C/70 °C District Heating Network Within the UoM MED

Pipe No.	Nodes		Length	Diameter	Heat transfer coefficient
	From	To	(m)	(mm)	(W/C)
1	0	12	40	219.10	0.4550
2	12	1	20	168.30	0.3670
3	12	13	70	219.10	0.4550
4	13	2	20	139.70	0.3670
5	13	14	70	219.10	0.4550
6	14	15	70	219.10	0.4550
7	15	5	130	219.10	0.4550
8	5	25	30	168.30	0.3670
9	5	16	80	114.30	0.3210
10	16	17	40	76.10	0.2780
11	17	4	20	48.30	0.2190
12	17	3	40	88.90	0.3270
13	25	19	20	60.30	0.2360
14	19	6	10	48.30	0.2190
15	19	7	30	60.30	0.2360
16	20	25	20	168.30	0.3670
17	20	9	20	168.30	0.3670
18	18	20	40	168.30	0.3670
19	22	18	20	168.30	0.3670
20	18	21	40	88.90	0.3270
21	21	8	40	88.90	0.3270
22	23	22	20	168.30	0.3670
23	24	23	20	219.10	0.4550
24	23	10	40	88.90	0.3270
25	11	24	100	219.10	0.4550
26	27	0	10	219.10	0.4550
27	26	11	10	219.10	0.4550

APPENDIX
THE UoM MED TEST CASE

This section provides a detailed description of the UoM MED test case used to demonstrate the different topics covered in this article. The information provided include the technical data required to simulate the integrated electricity–heat–gas network, as well as the energy profiles associated with the different buildings connected to the networks.

The UoM MED comprises 26 buildings with an annual electricity demand of 28 GWh (6-MW peak) and an annual heat demand of 18 GWh (12-MW peak). In addition, 13 additional buildings (39 buildings in total) share some of the networks with the district and thus must be considered when modeling the integrated electricity-heat-gas network. The integrated network, see Fig. 19, comprises: 1) the 22-bus 6.6-kV electricity distribution network presented in Table 1; 2) the 27-node 85 °C/70 °C (supply/return) district heating network presented in Table 2; and 3) the 36-node gas network presented in Table 3 [16]. In its base configuration: the slack nodes, denoted as nodes 0 in the respective networks, are connected to the electricity and gas supply points as well as with the largest boiler for the heat network; the MED imports electricity from the electricity grid (node 0), and produces heat with 19.2-, 18-, and 4.8-MW gas boilers connected to the nodes 0/0, 11/12, and 27/36 of the heat/gas networks. However, more in general this UoM MED system is meant to be used as a testbed for the simulation and optimization of alternative DER configurations, such as those illustrated in this article and in previous studies [16], [33]. For this purpose, the electricity, heat, and gas profiles (17 520 half hourly data points for a year) for each of the 26 buildings of the UoM MED as well as the additional 13 buildings connected to its energy networks (39 buildings in total) are provided in [128].

Table 3 Parameters of the 2 Bar Gas Network Within the UoM MED

Pipe No.	Nodes		Length	Diameter
	From	To	(m)	(mm)
1	15	0	240	100
2	15	34	220	100
3	34	18	320	100
4	18	13	90	100
5	34	35	260	100
6	35	16	90	100
7	16	17	20	100
8	17	1	20	500
9	17	2	80	100
10	35	32	160	500
11	32	33	20	500
12	32	19	180	500
13	19	14	110	500
14	33	22	20	500
15	22	21	150	100
16	21	4	30	100
17	4	5	90	100
18	21	20	20	100
19	20	3	20	100
20	22	23	200	100
21	23	24	60	100
22	24	6	20	100
23	24	7	20	500
24	33	25	90	100
25	25	26	130	100
26	26	11	20	500
27	26	27	40	100
28	27	9	20	100
29	27	28	40	100
30	28	10	100	100
31	28	29	40	100
32	29	8	20	100
33	30	29	20	100
34	30	31	200	100
35	31	12	110	100
36	36	15	100	100
37	15	0	240	100

REFERENCES

[1] R. Moreno, A. Street, J. M. Arroyo, and P. Mancarella, "Planning low-carbon electricity systems under uncertainty considering operational flexibility and smart grid technologies," *Phil. Trans. Roy. Soc. A, Math., Phys. Eng. Sci.*, vol. 375, no. 2100, Aug. 2017, Art. no. 20160305.

[2] P. Mancarella, "MES (multi-energy systems): An overview of concepts and evaluation models," *Energy*, vol. 65, pp. 1–17, Nov. 2014.

[3] N. Good, E. A. M. Ceseña, and P. Mancarella, "Ten questions concerning smart districts," *Building Environ.*, vol. 118, pp. 362–376, Jun. 2017.

[4] E. A. M. Ceseña, N. Good, M. Panteli, J. Mutale, and P. Mancarella, "Flexibility in sustainable electricity systems: Multivector and multisector nexus perspectives," *IEEE Electrific. Mag.*, vol. 7, no. 2, pp. 12–21, Jun. 2019.

[5] R. Jacob, M. Belusko, M. Liu, W. Saman, and F. Bruno, "Using renewables coupled with thermal energy storage to reduce natural gas consumption in higher temperature commercial/industrial applications," *Renew. Energy*, vol. 131, pp. 1035–1046, Feb. 2019.

[6] C. J. Quarton and S. Samsatli, "Power-to-gas for injection into the gas grid: What can we learn from real-life projects, economic assessments and systems modelling?" *Renew. Sustain. Energy Rev.*, vol. 98, pp. 302–316, Dec. 2018.

[7] M. Ban, J. Yu, M. Shahidehpour, and Y. Yao, "Integration of power-to-hydrogen in day-ahead security-constrained unit commitment with high wind penetration," *J. Mod. Power Syst. Clean Energy*, vol. 5, no. 3, pp. 337–349, May 2017.

[8] E. A. M. Ceseña, N. Good, A. L. A. Syrri, and P. Mancarella, "Techno-economic and business case assessment of multi-energy microgrids with co-optimization of energy, reserve and reliability services," *Appl. Energy*, vol. 210, pp. 896–913, Jan. 2018.

[9] G. Chicco, S. Riaz, A. Mazza, and P. Mancarella, "Flexibility from distributed multienergy systems," *Proc. IEEE*, to be published. [Online]. Available: https://ieeexplore-ieee-org.manchester.idm.oclc.org/document/9082595

[10] P. Mancarella, G. Andersson, J. A. Pecas-Lopes, and K. R. W. Bell, "Modelling of integrated multi-energy systems: Drivers, requirements, and opportunities," in *Proc. Power Syst. Comput. Conf. (PSCC)*, Jun. 2016, pp. 1–22.

[11] I. van Beuzekom, M. Gibescu, and J. G. Slootweg, "A review of multi-energy system planning and optimization tools for sustainable urban development," in *Proc. IEEE Eindhoven PowerTech*, Jun. 2015, pp. 1–7.

[12] N. Good, E. Karangelos, A. Navarro-Espinosa, and P. Mancarella, "Optimization under uncertainty of thermal storage-based flexible demand response with quantification of residential users' discomfort," *IEEE Trans. Smart Grid*, vol. 6, no. 5, pp. 2333–2342, Feb. 2015.

[13] E. A. M. Ceseña, N. Good, and P. Mancarella, "Energy efficiency at the building and district levels in a multi-energy context," in *Proc. IEEE Int. Energy Conf. (ENERGYCON)*, Apr. 2016, pp. 1–6.

[14] P. Meibom, J. Kiviluoma, R. Barth, H. Brand, C. Weber, and H. Larsen, "Value of electrical heat boilers and heat pumps for wind power integration," in *Proc. Eur. Wind Energy Conf. Exhib.*, 2006, vol. 10, no. 4, pp. 321–337.

[15] B. V. Mathiesen and H. Lund, "Comparative analyses of seven technologies to facilitate the integration of fluctuating renewable energy sources," *IET Renew. Power Gener.*, vol. 3, no. 2, p. 190, 2009.

[16] X. Liu and P. Mancarella, "Modelling, assessment and sankey diagrams of integrated electricity-heat-gas networks in multi-vector district energy systems," *Appl. Energy*, vol. 167, pp. 336–352, Apr. 2016.

[17] X. Liu, J. Wu, N. Jenkins, and A. Bagdanavicius, "Combined analysis of electricity and heat networks," *Appl. Energy*, vol. 162, pp. 1238–1250, Jan. 2016.

[18] A. G. Olabi, "Energy quadrilemma and the future of renewable energy," *Energy*, vol. 108, pp. 1–6, Aug. 2016.

[19] J. A. Sautter, J. Landis, and M. H. Dworkin, "The energy trilemma in the green mountain state: An analysis of Vermont's energy challenges and policy options," *Vermont J. Environ. Law*, vol. 10, no. 3, p. 477, 2009.

[20] S. Bahrami and A. Sheikhi, "From demand response in smart grid toward integrated demand response in smart energy hub," *IEEE Trans. Smart Grid*, vol. 7, no. 2, pp. 1–9, Aug. 2015.

[21] P. Mancarella and G. Chicco, "Real-time demand response from energy shifting in distributed multi-generation," *IEEE Trans. Smart Grid*, vol. 4, no. 4, pp. 1928–1938, Dec. 2013.

[22] A. F. Meyabadi and M. H. Deihimi, "A review of demand-side management: Reconsidering theoretical framework," *Renew. Sustain. Energy Rev.*, vol. 80, pp. 367–379, Dec. 2017.

[23] *Economy 7*. Accessed: Nov. 17, 2019. [Online]. Available: https://www.economyseven.co.uk/

[24] N. U. Hassan *et al.*, "Framework for minimum user participation rate determination to achieve specific demand response management objectives in residential smart grids," *Int. J. Electr. Power Energy Syst.*, vol. 74, pp. 91–103, Jan. 2016.

[25] E. A. M. Ceseña, N. Good, and P. Mancarella, "Electrical network capacity support from demand side response: Techno-economic assessment of potential business cases for small commercial and residential end-users," *Energy Policy*, vol. 82, pp. 222–232, Jul. 2015.

[26] M. Sun, Y. Wang, F. Teng, Y. Ye, G. Strbac, and C. Kang, "Clustering-based residential baseline estimation: A probabilistic perspective," *IEEE Trans. Smart Grid*, vol. 10, no. 6, pp. 6014–6028, Nov. 2019.

[27] V. Trovato, I. M. Sanz, B. Chaudhuri, and G. Strbac, "Advanced control of thermostatic loads for rapid frequency response in great Britain," *IEEE Trans. Power Syst.*, vol. 32, no. 3, pp. 2106–2117, May 2017.

[28] S. Althaher, P. Mancarella, and J. Mutale, "Automated demand response from home energy management system under dynamic pricing and power and comfort constraints," *IEEE Trans. Smart Grid*, vol. 6, no. 4, pp. 1874–1883, Jul. 2015.

[29] *Active Distribution Networks With Full Integration of Demand and Distributed Energy RESourceS*. Accessed: Nov. 14, 2019. [Online]. Available: http://www.addressfp7.org/

[30] A. Losi, P. Mancarella, and A. Vicino, *Integration of Demand Response Into the Electricity Chain: Challenges, Opportunities, and Smart Grid Solutions*. Hoboken, NJ, USA: Wiley, 2015.

[31] N. Good and P. Mancarella, "Flexibility in multi-energy communities with electrical and thermal storage: A stochastic, robust approach for multi-service demand response," *IEEE Trans. Smart Grid*, vol. 10, no. 1, pp. 503–513, Jan. 2019.

[32] E. A. M. Ceseña, T. Capuder, and P. Mancarella, "Flexible distributed multienergy generation system expansion planning under uncertainty," *IEEE Trans. Smart Grid*, vol. 7, no. 1, pp. 348–357, Jan. 2016.

[33] E. A. M. Ceseña and P. Mancarella, "Energy systems integration in smart districts: Robust optimisation of multi-energy flows in integrated electricity, heat and gas networks," *IEEE Trans. Smart Grid*, vol. 10, no. 1, pp. 1122–1131, Jan. 2019.

[34] X. Zhang, M. Shahidehpour, A. Alabdulwahab, and A. Abusorrah, "Optimal expansion planning of energy hub with multiple energy infrastructures," *IEEE Trans. Smart Grid*, vol. 6, no. 5, pp. 2302–2311, Sep. 2015.

[35] J. Keirstead and N. Shah, *Urban Energy Systems: An Integrated Approach*. New York, NY, USA: Taylor & Francis, 2013.

[36] M. Mohammadi, Y. Noorollahi, B. Mohammadi-Ivatloo, and H. Yousefi, "Energy hub: From a model to a concept—A review," *Renew. Sustain. Energy Rev.*, vol. 80, pp. 1512–1527, Dec. 2017.

[37] L. Ren *et al.*, "Enabling resilient distributed power sharing in networked microgrids through software defined networking," *Appl. Energy*, vol. 210, pp. 1251–1265, Jan. 2018.

[38] M. Yan, N. Zhang, X. Ai, M. Shahidehpour, C. Kang, and J. Wen, "Robust two-stage regional-district scheduling of multi-carrier energy systems with a large penetration of wind power," *IEEE Trans. Sustain. Energy*, vol. 10, no. 3, pp. 1227–1239, Jul. 2019.

[39] S. Clegg and P. Mancarella, "Integrated electricity-heat-gas modelling and assessment, with applications to the great britain system. Part II: Transmission network analysis and low carbon technology and resilience case studies," *Energy*, vol. 184, pp. 191–203, Oct. 2019.

[40] E. Fabrizio, V. Corrado, and M. Filippi, "A model to design and optimize multi-energy systems in buildings at the design concept stage," *Renew. Energy*, vol. 35, no. 3, pp. 644–655, Mar. 2010.

[41] T. Capuder and P. Mancarella, "Techno-economic and environmental modelling and optimization of flexible distributed multi-generation options," *Energy*, vol. 71, pp. 516–533, Jul. 2014.

[42] D. Zhang and D. Dechev, "A lock-free priority queue design based on multi-dimensional linked lists," *IEEE Trans. Parallel Distrib. Syst.*, vol. 27, no. 3, pp. 613–626, Mar. 2016.

[43] N. Amjady, S. Dehghan, A. Attarha, and A. J. Conejo, "Adaptive robust network-constrained AC unit commitment," *IEEE Trans. Power Syst.*, vol. 32, no. 1, pp. 672–683, Jan. 2017.

[44] Q. P. Zheng, J. Wang, and A. L. Liu, "Stochastic optimization for unit commitment—A review," *IEEE Trans. Power Syst.*, vol. 30, no. 4, pp. 1913–1924, Sep. 2015.

[45] N. Li, C. Uckun, E. M. Constantinescu, J. R. Birge, K. W. Hedman, and A. Botterud, "Flexible operation of batteries in power system scheduling with renewable energy," *IEEE Trans. Sustain. Energy*, vol. 7, no. 2, pp. 685–696, Apr. 2016.

[46] A. Monti, D. Pesch, K. A. Ellis, and P. Mancarella, *Energy Positive Neighborhoods and Smart Energy Districts: Methods, Tools, and Experiences from the Field*. Amsterdam, The Netherlands: Academic, 2017.

[47] National Grid. (2017). *Transmission Electricity Charges TNUoS Triad Data | National Grid*. Accessed: Mar. 27, 2017. [Online]. Available: http://www2.nationalgrid.com/UK/Industry-information/System-charges/Electricity-transmission/Transmission-Network-Use-of-System-Charges/Transmission-Charges-Triad-Data/

[48] N. Good, E. A. M. Ceseña, L. Zhang, and P. Mancarella, "Techno-economic and business case assessment of low carbon technologies in distributed multi-energy systems," *Appl. Energy*, vol. 167, pp. 158–172, Apr. 2016.

[49] Coherent Research. (2017). *Coherent Data Collection Server*. Accessed: Apr. 4, 2017. [Online]. Available: https://www.ems.estates.manchester.ac.uk/DCS/Logon.aspx?ReturnUrl=%2FDCS

[50] I. Richardson, M. Thomson, D. Infield, and C. Clifford, "Domestic electricity use: A high-resolution energy demand model," *Energy Buildings*, vol. 42, no. 10, pp. 1878–1887, Oct. 2010.

[51] R. Baetens *et al.*, "Assessing electrical bottlenecks at feeder level for residential net zero-energy buildings by integrated system simulation," *Appl. Energy*, vol. 96, pp. 74–83, Aug. 2012.

[52] N. Good, L. Zhang, A. Navarro-Espinosa, and P. Mancarella, "High resolution modelling of multi-energy domestic demand profiles," *Appl. Energy*, vol. 137, pp. 193–210, Jan. 2015.

[53] Y. Yamaguchi, S. Yilmaz, N. Prakash, S. K. Firth, and Y. Shimoda, "A cross analysis of existing methods for modelling household appliance use,"

J. Building Perform. Simul., vol. 12, no. 2, pp. 160–179, Mar. 2019.
[54] F. Lombardi, S. Balderrama, S. Quoilin, and E. Colombo, "Generating high-resolution multi-energy load profiles for remote areas with an open-source stochastic model," *Energy*, vol. 177, pp. 433–444, Jun. 2019.
[55] *Ofgem*. Accessed: Feb. 27, 2020. [Online]. Available: https://www.ofgem.gov.uk/
[56] E. Loukarakis, C. J. Dent, and J. W. Bialek, "Decentralized multi-period economic dispatch for real-time flexible demand management," *IEEE Trans. Power Syst.*, vol. 31, no. 1, pp. 672–684, Jan. 2016.
[57] S. Clegg and P. Mancarella, "Storing renewables in the gas network: Modelling of power-to-gas seasonal storage flexibility in low-carbon power systems," *IET Gener., Transmiss. Distrib.*, vol. 10, no. 3, pp. 566–575, Feb. 2016.
[58] S. Clegg and P. Mancarella, "Integrated modeling and assessment of the operational impact of power-to-gas (P2G) on electrical and gas transmission networks," *IEEE Trans. Sustain. Energy*, vol. 6, no. 4, pp. 1234–1244, Oct. 2015.
[59] T. Li, M. Eremia, and M. Shahidehpour, "Interdependency of natural gas network and power system security," *IEEE Trans. Power Syst.*, vol. 23, no. 4, pp. 1817–1824, Nov. 2008.
[60] M. Shahidehpour, Y. Fu, and T. Wiedman, "Impact of natural gas infrastructure on electric power systems," *Proc. IEEE*, vol. 93, no. 5, pp. 1042–1056, May 2005.
[61] J. Fang, Q. Zeng, X. Ai, Z. Chen, and J. Wen, "Dynamic optimal energy flow in the integrated natural gas and electrical power systems," *IEEE Trans. Sustain. Energy*, vol. 9, no. 1, pp. 188–198, Jan. 2018.
[62] C. Liu, M. Shahidehpour, and J. Wang, "Coordinated scheduling of electricity and natural gas infrastructures with a transient model for natural gas flow," *Chaos, Interdiscipl. J. Nonlinear Sci.*, vol. 21, no. 2, Jun. 2011, Art. no. 025102.
[63] T. Capuder and P. Mancarella, "Assessing the benefits of coordinated operation of aggregated distributed multi-energy generation," in *Proc. Power Syst. Comput. Conf. (PSCC)*, Jun. 2016, pp. 1–7.
[64] A. Shabanpour-Haghighi and A. R. Seifi, "An integrated steady-state operation assessment of electrical, natural gas, and district heating networks," *IEEE Trans. Power Syst.*, vol. 31, no. 5, pp. 3636–3647, Sep. 2016.
[65] S. Clegg and P. Mancarella, "Integrated electrical and gas network flexibility assessment in low-carbon multi-energy systems," *IEEE Trans. Sustain. Energy*, vol. 7, no. 2, pp. 718–731, Apr. 2016.
[66] P. Wong and R. Larson, "Optimization of natural-gas pipeline systems via dynamic programming," *IEEE Trans. Autom. Control*, vol. 13, no. 5, pp. 475–481, Oct. 1968.
[67] A. Martinez-Mares and C. R. Fuerte-Esquivel, "A unified gas and power flow analysis in natural gas and electricity coupled networks," *IEEE Trans. Power Syst.*, vol. 27, no. 4, pp. 2156–2166, Nov. 2012.
[68] M. Geidl and G. Andersson, "Optimal power flow of multiple energy carriers," *IEEE Trans. Power Syst.*, vol. 22, no. 1, pp. 145–155, Feb. 2007.
[69] M. Moeini-Aghtaie, A. Abbaspour, M. Fotuhi-Firuzabad, and E. Hajipour, "A decomposed solution to multiple-energy carriers optimal power flow," *IEEE Trans. Power Syst.*, vol. 29, no. 2, pp. 707–716, Mar. 2014.
[70] M. Qadrdan, J. Wu, N. Jenkins, and J. Ekanayake, "Operating strategies for a GB integrated gas and electricity network considering the uncertainty in wind power forecasts," *IEEE Trans. Sustain. Energy*, vol. 5, no. 1, pp. 128–138, Jan. 2014.
[71] C. Liu, M. Shahidehpour, Y. Fu, and Z. Li, "Security-constrained unit commitment with natural gas transmission constraints," *IEEE Trans. Power Syst.*, vol. 24, no. 3, pp. 1523–1536, Aug. 2009.
[72] A. J. Osiadacz, *Simulation and Analysis of Gas Networks*. London, U.K.: Spon, 1987.
[73] E. S. Menon, *Gas Pipeline Hydraulics*. Boca Raton, FL, USA: CRC Press, 2005.
[74] B. Larock, R. Jeppson, and G. Watters, *Hydraulics of Pipeline Systems*. Boca Raton, FL, USA: CRC Press, 1999.
[75] E. S. Menon, *Liquid Pipeline Hydraulics*. Boca Raton, FL, USA: CRC Press, 2004.
[76] X. Liu, J. Wu, N. Jenkins, and A. Bagdanavicius, "Combined analysis of electricity and heat networks," *Appl. Energy*, vol. 162, pp. 1238–1250, Jan. 2016.
[77] X. S. Jiang, Z. X. Jing, Y. Z. Li, Q. H. Wu, and W. H. Tang, "Modelling and operation optimization of an integrated energy based direct district water-heating system," *Energy*, vol. 64, pp. 375–388, Jan. 2014.
[78] G. Sandou *et al.*, "Predictive control of a complex district heating network," in *Proc. 44th IEEE Conf. Decis. Control, Eur. Control Conf. (CDC-ECC)*, 2005, p. 7372.
[79] E. Ikonen *et al.*, "Short term optimization of district heating network supply temperatures," in *Proc. IEEE Int. Energy Conf. (ENERGYCON)*, May 2014, pp. 996–1003.
[80] P. Jie, Z. Tian, S. Yuan, and N. Zhu, "Modeling the dynamic characteristics of a district heating network," *Energy*, vol. 39, no. 1, pp. 126–134, Mar. 2012.
[81] *Official DIMMER—District Information Modeling and Management for Energy Reduction Project Kickoff | Istituto Superiore Mario Boella*. Accessed: Nov. 16, 2019. [Online]. Available: http://www.ismb.it/en/node/2174
[82] E. Patti, A. Ronzino, A. Osello, V. Verda, A. Acquaviva, and E. Macii, "District information modeling and energy management," *IT Prof.*, vol. 17, no. 6, pp. 28–34, Nov. 2015.
[83] E. A. M. Ceseña and P. Mancarella, "Distribution network support from multi-energy demand side response in smart districts," in *Proc. IEEE Innov. Smart Grid Technol.-Asia (ISGT-Asia)*, Nov. 2016, pp. 1–6.
[84] B. van der Heijde *et al.*, "Dynamic equation-based thermo-hydraulic pipe model for district heating and cooling systems," *Energy Convers. Manage.*, vol. 151, pp. 158–169, Nov. 2017.
[85] A. Vandermeulen, B. van der Heijde, and L. Helsen, "Controlling district heating and cooling networks to unlock flexibility: A review," *Energy*, vol. 151, pp. 103–115, May 2018.
[86] S. Verbeke and A. Audenaert, "Thermal inertia in buildings: A review of impacts across climate and building use," *Renew. Sustain. Energy Rev.*, vol. 82, pp. 2300–2318, Feb. 2018.
[87] N. Good, K. A. Ellis, and P. Mancarella, "Review and classification of barriers and enablers of demand response in the smart grid," *Renew. Sustain. Energy Rev.*, vol. 72, pp. 57–72, May 2017.
[88] A. Boardman, S. Mockford, and P. Lawson, *Guidance for the Application of ENA ER P2/6 Security of Supply*, Standard EDS 08-0119, 2014.
[89] G. Mavromatidis *et al.*, "Ten questions concerning modeling of distributed multi-energy systems," *Building Environ.*, vol. 165, Nov. 2019, Art. no. 106372.
[90] S. Chen and C.-C. Liu, "From demand response to transactive energy: State of the art," *J. Mod. Power Syst. Clean Energy*, vol. 5, no. 1, pp. 10–19, Jan. 2017.
[91] S. Chen, Z. Wei, G. Sun, K. W. Cheung, and Y. Sun, "Multi-linear probabilistic energy flow analysis of integrated electrical and natural-gas systems," *IEEE Trans. Power Syst.*, vol. 32, no. 3, pp. 1970–1979, May 2017.
[92] Y. Wang *et al.*, "Operation optimization of regional integrated energy system based on the modeling of electricity-thermal-natural gas network," *Appl. Energy*, vol. 251, Oct. 2019, Art. no. 113410.
[93] S. Karamdel and M. P. Moghaddam, "Robust expansion co-planning of electricity and natural gas infrastructures for multi energy-hub systems with high penetration of renewable energy sources," *IET Renew. Power Gener.*, vol. 13, no. 13, pp. 2287–2297, Oct. 2019.
[94] L. G. Lagos and L. Ochoa, "WP2 deliverable 2.2: Assessment of LV interconnection benefits for different LCT penetrations," Univ. Manchester, Manchester, U.K., Tech. Rep. 2T2.2_D2.2.2, 2016.
[95] A. Navarro-Espinosa and P. Mancarella, "Probabilistic modeling and assessment of the impact of electric heat pumps on low voltage distribution networks," *Appl. Energy*, vol. 127, pp. 249–266, Aug. 2014.
[96] H. Wang, A. Saint-Pierre, and P. Mancarella, "System level cost and environmental performance of integrated energy systems: An assessment of low-carbon scenarios for the UK," in *Proc. IEEE Eindhoven PowerTech*, Jun. 2015, pp. 1–6.
[97] H. Wang and P. Mancarella, "Towards sustainable urban energy systems: High resolution modelling of electricity and heat demand profiles," in *Proc. IEEE Int. Conf. Power Syst. Technol. (POWERCON)*, Sep. 2016, pp. 1–6.
[98] *Multi-Energy Storage-Social, TechnO-Economic, Regulatory and Environmental assessment under uncertainty*. Accessed: Nov. 16, 2019. [Online]. Available: https://gow.epsrc.ukri.org/NGBOViewGrant.aspx?GrantRef=EP/N001974/1
[99] *Triad Guidance Notes*, Flexitricity, Edinburgh, Scotland, 2010.
[100] A. W. Dowling, R. Kumar, and V. M. Zavala, "A multi-scale optimization framework for electricity market participation," *Appl. Energy*, vol. 190, pp. 147–164, Mar. 2017.
[101] ENWL. (2017). *Managed Connections*. Accessed: Apr. 1, 2017. [Online]. Available: http://www.enwl.co.uk/our-services/connection-services/generation/managed-connections
[102] J. A. Schachter, P. Mancarella, J. Moriarty, and R. Shaw, "Flexible investment under uncertainty in smart distribution networks with demand side response: Assessment framework and practical implementation," *Energy Policy*, vol. 97, pp. 439–449, Oct. 2016.
[103] Electricity Northwest. *Capacity to Customers (C2C) Project*. Accessed: Apr. 5, 2017. [Online]. Available: http://www.enwl.co.uk/c2c
[104] ENWL. *Smart Street*. Accessed: Nov. 17, 2019. [Online]. Available: https://www.enwl.co.uk/zero-carbon/our-key-innovation-projects/smart-street/
[105] E. A. M. Ceseña and P. Mancarella, "Practical recursive algorithms and flexible open-source applications for planning of smart distribution networks with demand response," *Sustain. Energy, Grids Netw.*, vol. 7, pp. 104–116, Sep. 2016.
[106] L. Zhang, T. Capuder, and P. Mancarella, "Unified unit commitment formulation and fast multi-service LP model for flexibility evaluation in sustainable power systems," *IEEE Trans. Sustain. Energy*, vol. 7, no. 2, pp. 658–671, Apr. 2016.
[107] P. Mancarella *et al.*, "Power system security assessment of the future National Electricity Market," Melbourne Energy Inst., Melbourne, VIC, Australia, Tech. Rep., 2017. [Online]. Available: https://www.energy.gov.au/sites/default/files/independent-review-future-nem-power-system-security-assessment.pdf
[108] C. Eid, P. Codani, Y. Perez, J. Reneses, and R. Hakvoort, "Managing electric flexibility from distributed energy resources: A review of incentives for market design," *Renew. Sustain. Energy Rev.*, vol. 64, pp. 237–247, Oct. 2016.
[109] N. Good, E. A. M. Ceseña, C. Heltorp, and P. Mancarella, "A transactive energy modelling and assessment framework for demand response business cases in smart distributed multi-energy systems," *Energy*, vol. 184, pp. 165–179, Oct. 2019.
[110] N. Good and P. Mancarella, "Modelling and assessment of business cases for smart multi-energy districts," in *Proc. PSCC*, Jun. 2016, pp. 1–7.
[111] G. Chicco and P. Mancarella, "From cogeneration to trigeneration: Profitable alternatives in a competitive market," *IEEE Trans. Energy Convers.*,

vol. 21, no. 1, pp. 265–272, Mar. 2006.
[112] A. Majzoobi and A. Khodaei, "Application of microgrids in providing ancillary services to the utility grid," *Energy*, vol. 123, pp. 555–563, Mar. 2017.
[113] L. Zhang, N. Good, and P. Mancarella, "Building-to-grid flexibility: Modelling and assessment metrics for residential demand response from heat pump aggregations," *Appl. Energy*, vols. 233–234, pp. 709–723, Jan. 2019.
[114] F. Scheller, B. Burgenmeister, H. Kondziella, S. Kühne, D. G. Reichelt, and T. Bruckner, "Towards integrated multi-modal municipal energy systems: An actor-oriented optimization approach," *Appl. Energy*, vol. 228, pp. 2009–2023, Oct. 2018.
[115] E. A. M. Ceseña, V. Turnham, and P. Mancarella, "Regulatory capital and social trade-offs in planning of smart distribution networks with application to demand response solutions," *Electr. Power Syst. Res.*, vol. 141, pp. 63–72, Dec. 2016.
[116] ESC. *Modern Energy Partners*. Accessed: Nov. 16, 2019. [Online]. Available: https://es.catapult.org.uk/service-platforms/modern-energy-partners/
[117] D. Norman and K. van Alphen. (2020). *Enabling the Decarbonisation of Australia's Energy Networks*. Accessed: Mar. 6, 2020. [Online]. Available: https://www.futurefuelscrc.com/
[118] R. Gupta. (2019). *Multi Energy Vector Modelling | NIA_NGTO037 | Smarter Networks*. Accessed: Mar. 6, 2020. [Online]. Available: https://www.smarternetworks.org/project/nia_ngto037/print
[119] M. Panteli, P. Mancarella, D. N. Trakas, E. Kyriakides, and N. D. Hatziargyriou, "Metrics and quantification of operational and infrastructure resilience in power systems," *IEEE Trans. Power Syst.*, vol. 32, no. 6, pp. 4732–4742, Nov. 2017.
[120] C. Shao, M. Shahidehpour, X. Wang, X. Wang, and B. Wang, "Integrated planning of electricity and natural gas transportation systems for enhancing the power grid resilience," *IEEE Trans. Power Syst.*, vol. 32, no. 6, pp. 4418–4429, Nov. 2017.
[121] M. Panteli, C. Pickering, S. Wilkinson, R. Dawson, and P. Mancarella, "Power system resilience to extreme weather: Fragility modeling, probabilistic impact assessment, and adaptation measures," *IEEE Trans. Power Syst.*, vol. 32, no. 5, pp. 3747–3757, Sep. 2017.
[122] Y. Zhou, M. Panteli, R. Moreno, and P. Mancarella, "System-level assessment of reliability and resilience provision from microgrids," *Appl. Energy*, vol. 230, pp. 374–392, Nov. 2018.
[123] E. Loukarakis, J. W. Bialek, and C. J. Dent, "Investigation of maximum possible OPF problem decomposition degree for decentralized energy markets," *IEEE Trans. Power Syst.*, vol. 30, no. 5, pp. 2566–2578, Sep. 2015.
[124] E. Dall'Anese, P. Mancarella, and A. Monti, "Unlocking flexibility: Integrated optimization and control of multienergy systems," *IEEE Power Energy Mag.*, vol. 15, no. 1, pp. 43–52, Jan. 2017.
[125] E. Patti, A. L. A. Syrri, M. Jahn, P. Mancarella, A. Acquaviva, and E. Macii, "Distributed software infrastructure for general purpose services in smart grid," *IEEE Trans. Smart Grid*, vol. 7, no. 2, pp. 1156–1163, Mar. 2016.
[126] D. Xu *et al.*, "Distributed multienergy coordination of multimicrogrids with biogas-solar-wind renewables," *IEEE Trans. Ind. Informat.*, vol. 15, no. 6, pp. 3254–3266, Jun. 2019.
[127] Z. Liu, Q. Wu, S. Huang, and H. Zhao, "Transactive energy: A review of state of the art and implementation," in *Proc. IEEE Manchester PowerTech*, Jun. 2017, pp. 1–6.
[128] E. A. M. Ceseña, E. Loukarakis, N. Good, and P. Mancarella. (2020). Multi-Energy District and Multi-Energy Network Test Case. University of Manchester. [Online]. Available: https://www.researchgate.net/publication/339768593_UOM_MED

ABOUT THE AUTHORS

Eduardo Alejandro Martínez Ceseña (Member, IEEE) received the M.Sc. degree in power systems from the Instituto Tecnológico de Morelia, Morelia, Mexico, in 2008, and the Ph.D. degree in power systems from The University of Manchester, Manchester, U.K., in 2012.

He is currently an Academic Fellow with the Department of Electrical and Electronic Engineering, The University of Manchester. His research interests include the planning and design of electricity infrastructure under uncertainty (e.g., photovoltaic (PV) systems, wind farms, and distribution networks), power system economics, optimization techniques and, especially, planning of community multienergy systems in consideration of integrated electricity–heat–gas networks and local and system level needs.

Emmanouil Loukarakis received the Ph.D. degree on power systems from Durham University, Durham, U.K., in 2016.

He has previously worked as a Postdoctoral Researcher for The University of Manchester, Manchester, U.K., focusing on the area of multienergy systems modeling and optimization. He is currently working for Levelise Ltd., Oxford, U.K., as an Operations Research Scientist. His research interests include power system design, control, and economics.

Nicholas Good received the Ph.D. degree in electrical engineering from The University of Manchester, Manchester, U.K., in 2015.

He is currently a Researcher and a Data Scientist at Upside Energy Ltd., Manchester, U.K., a provider of software to monitor, forecast, optimize, trade, dispatch, and analyze distributed energy resources. He maintains a research interest in optimization of flexible multienergy systems under uncertainty and associated business case development.

Pierluigi Mancarella (Senior Member, IEEE) received the M.Sc. and Ph.D. degrees in electrical energy systems from the Politecnico di Torino, Turin, Italy, in 2002 and 2006, respectively.

He is currently the Chair Professor of electrical power systems with The University of Melbourne, Melbourne, VIC, Australia, and a Professor of smart energy systems with The University of Manchester, Manchester, U.K. His research interests include multienergy systems, power system integration of low-carbon technologies, network planning under uncertainty, and risk and resilience of smart grids.

Dr. Mancarella is an Editor of the IEEE TRANSACTIONS ON POWER SYSTEMS and the IEEE TRANSACTIONS ON SMART GRID, an Associate Editor of the IEEE SYSTEMS JOURNAL, and an IEEE Power and Energy Society Distinguished Lecturer.